ETCHING OF GALLIUM ARSENIDE WITH ATOMIC HYDROGEN

By

John W. Elzey

A.B., University of California, Berkeley, 1990

A THESIS SUBMITTED IN PARTIAL FULFILLMENT OF

THE REQUIREMENTS FOR THE DEGREE OF

MASTER OF SCIENCE

in

THE FACULTY OF GRADUATE STUDIES

Department of Physics

We accept this thesis as conforming

to the required standard

THE UNIVERSITY OF BRITISH COLUMBIA

December 1992

© John W. Elzey, 1992

In presenting this thesis in partial fulfilment of the requirements for an advanced degree at the University of British Columbia, I agree that the Library shall make it freely available for reference and study. I further agree that permission for extensive copying of this thesis for scholarly purposes may be granted by the head of my department or by his or her representatives. It is understood that copying or publication of this thesis for financial gain shall not be allowed without my written permission.

(Signature)

Department of Physics

The University of British Columbia
Vancouver, Canada

Date Dec. 31, 1992

DE-6 (2/88)

Abstract

An optical interferometric method is used to make *in-situ* observations of continuous etching of the (100) GaAs surface during exposure to a known concentration of thermalised hydrogen atoms downstream from an H_2 plasma. Etch rates between 3 and 9 nm/min are followed at constant temperature within the range 229 - 360 °C. Increasing substrate temperature leads to increased rates of reaction. A Pt wire is used as an isothermal calorimeter to determine absolute H atom partial pressures on the order of 5 mTorr. Analysis of etch rate dependence on atomic hydrogen concentration verifies the surface reaction follows close to a first order rate law with respect to the hydrogen atom concentration and an Arrhenius analysis of the etch rate data yields an activation energy of 7(2) kcal/mol = 29(7) kJ/mol = 0.31(7) eV. Rate coefficients for the H + GaAs etching reaction were found in the aforementioned temperature range to have the temperature dependence $k_T = 10^{5.7\pm0.7}$ nm min^{-1} Torr^{-1} exp(-29±7 kJ/mol)/RT. Scanning electron microscope photomicrographs of etched samples reveal that large scale crystallographic etching occurs resulting in textured (100) GaAs surfaces and x-ray photoelectron spectroscopy demonstrated these surfaces were gallium-rich.

Table of Contents

Abstract.....ii

Table of Contents.....iii

List of Tables.....v

List of Figures.....vi

Acknowledgments.....vii

Section 1: Introduction.....1

1.1 General Purpose of Study.....1

1.2 Hydrogen Atoms in Silicon.....2

1.2.1 Atomic H on the Silicon Surface.....2

1.2.2 Atomic H Diffusion in Silicon.....2

1.2.3 Atomic H Generated Platelets in Silicon.....3

1.2.4 Atomic H Etching of Silicon.....4

1.3 Hydrogen Atoms in Gallium Arsenide.....4

1.3.1 Atomic H on the Gallium Arsenide Surface.....4

1.3.2 Atomic H Diffusion in Gallium Arsenide.....5

1.3.3 Atomic H Generated Platelets in Gallium Arsenide.....7

1.3.4 H2 Adsorption on Gallium Arsenide.....8

1.3.5 Atomic H Etching of Gallium Arsenide.....8

Section 2: Experimental.....14

2.1 Reaction Vessel.....14

2.2 Sample Holder and Thermometry.....18

2.3 Gallium Arsenide Samples and Silicon Nitride Mask.....20

2.4 Hydrogen Atom Production.....22

2.5 Hydrogen Atom Detection....23

2.6 Interferometer....27

Section 3: Results....35

3.1 Measurement of the Atomic Hydrogen Concentration....35

3.2 Measurement of the Order of the Reaction with Respect to the Concentration of Atomic Hydrogen....36

3.3 Measurement of the Absolute Rate Constants and Activation Energy for Etching Gallium Arsenide with Atomic Hydrogen....38

3.4 Post-etch Surface Description....41

3.5 X-Ray Photoelectron Spectroscopy Result....44

Section 4: Discussion....48

4.1 Atomic Hydrogen Adsorption on Silicon and Gallium Arsenide..48

4.2 Atomic Hydrogen Platelets in Gallium Arsenide....48

4.3 Atomic Hydrogen Induced Crystallographic Etching....49

Section 5: Conclusion....51

Suggestions for Further Work....52

References....54

Appendix 1: Slope Uncertainty Calculations....55

Appendix 2: Preexponential and Uncertainty Determination....58

List of Tables

Table 3-1 Atomic Hydrogen Reaction with Gallium Arsenide Order Estimate at 280 °C 37

Table 3-2 Atomic Hydrogen Reaction with Gallium Arsenide Order Estimate at 250 °C 37

Table 3-3 Measured Kinetic Quantities for the Hydrogen Atom Reaction with Gallium Arsenide and Subsequent Rate Constants 42

List of Figures

Figure 1-1 T_{III} and T_V tetrahedral and bond center sites for atomic hydrogen in GaAs (from L. Pavesi and P. Giannozzi[55]).....6

Figure 2-1 Schematic layout of etching reactor and monitor system.....15

Figure 2-2 Pyrex sample holder.....19

Figure 2-3 Silicon nitride stripe orientation on (100) GaAs.....21

Figure 2-4 Platinum wire configuration for H atom detection in flow system.....24

Figure 2-5 Schematic of Wheatstone bridge used with Pt wire to measure the partial pressure of hydrogen.....25

Figure 2-6 One period of a typical interferogram obtained during H atom etching of (100) GaAs at 281 °C.....30

Figure 2-7 Calculated Interferometer angular dependent intensity profile.....32

Figure 3-1 Plot of ln(GaAs Etch Rate) vs. ln(Hydrogen Atom Partial Pressure) at (a) 250 °C and (b) 280 °C to Estimate Reaction Order.....38

Figure 3-2 Arrhenius plot for the determination of the activation energy for the etching of GaAs with atomic hydrogen.....43

Figure 3-3 SEM photomicrographs of (100) GaAs etched at 205 °C from (a) side and (b) surface normal.....45

Figure 3-4 SEM photomicrographs of (100) GaAs etched at (a) 180 °C and (b) 205 C from surface normal.....46

Figure 3-5 SEM photomicrographs of (100) GaAs etched at (a) 280 °C and (b) 360 °C from side.....47

Figure A-1 Slope Uncertainty Estimate Illustration.....59

Figure A-2 Preexponential Determination with Uncertainty.....62

Acknowledgments

Thanks very much to the Mechanical Shop staff for friendly service and to Sean Adams for effective and conscientious glass blowing. Mary Mager in the Metallurgical Engineering Department also proved very helpful and must be credited for the good SEM shots. Hiroshi Kato in Electrical Engineering was an excellent guide in the fab lab and did much of the mask depositing work for me. I must also express my gratitude to Kin-Chung Wong for daily help during my introduction to this brand of experimental science. The extended loan of Physica B **170** 1991 from Rob Kiefl was very helpful as well as several conversations. Thanks too to George Y. Gu who I remember one day, aside from other support and help, blew many glass sample holders as fast as I could break them. Hongjun Li has also helped me struggle over various conceptual barriers. Ed Wishnow kindly shared his interferometer experience with me. I've greatly benefited from conversations with Paul Meharg. I am lucky to work with such a capable person willing to spend his time and brain cells explaining to me the details of what perhaps could have been only a section in *his* Ph.D. thesis. I *greatly* appreciate the patience of Dr. E. A. Ogryzlo.

SECTION 1: INTRODUCTION

1.1 GENERAL PURPOSE OF STUDY

It is scientifically and industrially relevant to understand the effects, including bonding details, of atomic hydrogen in and on GaAs. A myriad of compound semiconductor bipolar and field effect transistors as well as lasers are currently fabricated with the aid of various dry etching techniques[1] most of which contain hydrogen. An understanding of the behavior of H in one crystal should elucidate information relative to other perhaps more complicated crystals. Furthering the understanding of surface chemistry will undoubtedly result in improvements in device fabrication technology.

Hydrogen atoms are commonly present, intentionally and unintentionally in cleaning, growth, doping, neutralization and passivation of industrially prepared GaAs. GaAs permeates the whole of the optoelectronics industry and the review by Johnson et al[2] of experimental results of hydrogen in crystalline semiconductors displays the void in the mere determination of the binding energy parameter for hydrogen in GaAs.

The etching reaction of thermalised H atoms with gallium arsenide is of fundamental nature. Today, gas - solid reactions remain illusive to the theorist. The only first principles theoretical model which the author is aware of that successfully achieves etching of a semiconductor (Si) with a gas phase species (F) makes the approximation that the reaction occurs adiabatically[3] (i.e. no heat is carried away from the substrate).

The objectives of the current study are to demonstrate that thermalised atomic hydrogen does etch GaAs, to estimate the activation energy for such a process and to measure the absolute rate at which H etches GaAs. To our knowledge there have been no published estimates of the absolute rate constants for this etching reaction.

Measurement of the absolute hydrogen atom concentration separates the present work from non-kinetic studies of atomic hydrogen with semiconductors. It is hoped that someday theorists can reconcile the data of this experiment with others and provide a bona fide theory of the interaction of a semiconductor with the ever-present, simplest of atoms: hydrogen.

1.2 HYDROGEN ATOMS IN SILICON

1.2.1 ATOMIC HYDROGEN ON THE SILICON SURFACE

Atomic hydrogen saturates dangling bonds on silicon surfaces and tends to remove the reconstruction[4]. At room temperature both SiH and SiH_2 are formed on the Si surface. This can only be achieved through the breaking of Si-Si bonds. At 300 °C the SiH species dominates. Even molecular hydrogen dissociates enough at this temperature to promote H atom chemisorption which can hamper growth of epitaxial Si and SiGe films.

1.2.2 ATOMIC HYDROGEN DIFFUSION IN SILICON

Some convergence of theoretical and experimental studies exists today regarding the lowest energy configuration of atomic hydrogen in crystalline silicon. Electron paramagnetic resonance, muon spin resonance experiments show that the lowest energy configuration of H in silicon is the bond center (BC) position and there exists a secondary minimum for H at the antibonding site[4] (i.e. at a site a comparable distance from the Si atom as the bond centre, but on the opposite side of the Si atom).

Atomic hydrogen produced by a remote H_2 plasma is well known to diffuse into Si at moderate temperatures (150 - 300 °C)[5]. Hydrogen plasma exposure is usually achieved via either a radio frequency discharge (13.56 MHz) or a low frequency discharge (30 KHz). Of the several states in which H exists in the Si lattice

the BC site appears to be the most energetically favourable, particularly if lattice relaxation is possible, as it is close to a surface.[6]

The diffusion coefficient of H in Si was experimentally determined by Van Wieringen and Warmoltz[7] to be:

$$D = 9.4 \times 10^{-3} \exp(-11 \text{ kcal}/RT) \text{ cm}^2/\text{sec}$$

The solubility, S, of H in Si for 1 atmosphere of H was also found by Van Wieringen and Warmoltz to be:

$$S = 2.4 \times 10^{21} \exp(-43 \text{ kcal}/RT) \text{ molecules}/\text{cm}^3$$

$\sim 10^{-10}$ molecules/cm^3 at room temperature. Experiments detect far more atoms than this very low equilibrium value.

1.2.3 ATOMIC HYDROGEN GENERATED PLATELETS IN SILICON

Atomic hydrogen incorporation as a result of exposure to a remote H_2 plasma often leads to creation of extended defects. Johnson et al[8]. observed platelet (d_{avg} = 7 nm ~ 400 Si-H bonds) or microcrack formation (predominately along the {111} crystallographic planes and less than 0.1 μm from the surface) with transmission electron microscopy (TEM) in crystalline Si after exposure to high concentrations of atomic deuterium substituted for hydrogen. Johnson et al. found the density of platelets to be proportional to the near surface concentration of atomic deuterium. The H generated platelets can be thought of as discs of bonded H atom separating adjacent planes of a lattice.

Johnson et al.[8] concluded platelet formation in crystalline Si is due merely to diffusion of H into the crystal; not plasma or radiation damage. The first 5 nm of Si becomes "virtually amorphous"[9] while the first 200 nm suffers "severe crystalline disorder" revealed through cross sectional TEM for H plasma treated Si crystals.

Results of total energy calculations of H in Si lead Jackson and Zhang[10] to postulate that a paired form of H may be responsible for the formation of this

platelet effect. J. B. Boyce et. al.[11] performed nuclear magnetic resonance on dueterated crystalline silicon and obtained results consistent with the calculations of Jackson and Zhang. Hydrogen related platelets in silicon can now be attributed to the formation and clustering of what is commonly referred to as H_2^*, that is; pairs of atomic hydrogen are thought to enter Si - Si bonds by one of the H atoms breaking the Si - Si bond and simultaneously restoring full coordination of that Si atom, while the other H atom is thought to occupy the antibonding, tetrahedral interstitial position of the neighboring Si atom. Boyce, Johnson, Ready and Walker[11] successfully used NMR on deuterated (100) Si to observe the <111> orientation of the Si-D bonds in similar D-containing platelets. The resulting platelets are aligned along the {111} planes.

1.2.4 ATOMIC HYDROGEN ETCHING OF SILICON

Feng and Oehrlein[12] experimentally investigated the H atom etching of silicon in 1987. The above brief description of H atoms breaking Si-Si bonds (§ 1.2.1) close to the Si surface has been computationally confirmed to be plausible and suspected responsible for H atom etching of the {111}, {110} and {100} planes of crystalline Si[13] SiH_2 is found to desorb from the 16-atom cluster after a total of five zero-energy H atoms (one of which gives the surface Si atom full tetrahedral coordination) are incident upon it.

1.3 HYDROGEN ATOMS IN GALLIUM ARSENIDE

1.3.1 HYDROGEN ATOMS ON THE GALLIUM ARSENIDE SURFACE

H atom chemisorption on the (110) face of GaAs has been observed using electron energy loss spectroscopy[14] after exposing the (110) GaAs surface to H atoms from hot filament dissociated H_2. H is found to form covalent bonds with both the

Ga and the As atoms. Synchrotron radiation photoemission spectra[14] found As p-like and Ga and As s-like empty states on the (110) GaAs.

1.3.2 ATOMIC HYDROGEN DIFFUSION IN GALLIUM ARSENIDE

B. Clerjaud et al[15]. hypothesized that atomic hydrogen diffuses as either a neutral or a negatively charged species in SI GaAs.

The diffusion activation energy for H^0 in undoped GaAs was found by Rhabi et al[16] to be 0.97 eV.

In 1991 Johnson[17] stated there has been no direct determination of the existence of H_2 in a crystalline semiconductor. Most researchers believe however: "...the most stable form of H in semiconductors is the H_2 molecule."[18]

Molecular hydrogen may be present in hydrogenated GaAs, but H_2 is thought to be immobile, nearly inert and to reside at a site in GaAs with tetrahedral symmetry, with respect to nearest neighbors (e.g. between four "neighboring" As atoms), known as the T site[19] as shown in Figure 1-1.

There is another hydrogen complex, called H_2^*, consisting of one H in the BC site and a second H in the T site. H_2^* formation is suspected to aid H diffusion in GaAs as well as hopping between T sites[20]. Figure 1-1, from L. Pavesi and P. Giannozzi,[21] shows the various high symmetry sites in the GaAs lattice.

Secondary Ion Mass Spectrometry (SIMS) profiling preceded by deuteration appears to be the definitive technique for the determination of diffusion depth of H into a crystalline semiconductor. The solubility of H in GaAs appears to be 2×10^{20} H/cm^3.[22] Chevallier et al[23]. found in undoped GaAs the deuterium diffusion profile to be close to an error function and a diffusion coefficient for D three times larger in undoped samples than that of heavily Si-doped GaAs.

E. M. Omeljanovsky et al.[24] determined the temperature dependence of the diffusion coefficient of atomic hydrogen in Semi-Insulating GaAs to be D = 0.02exp

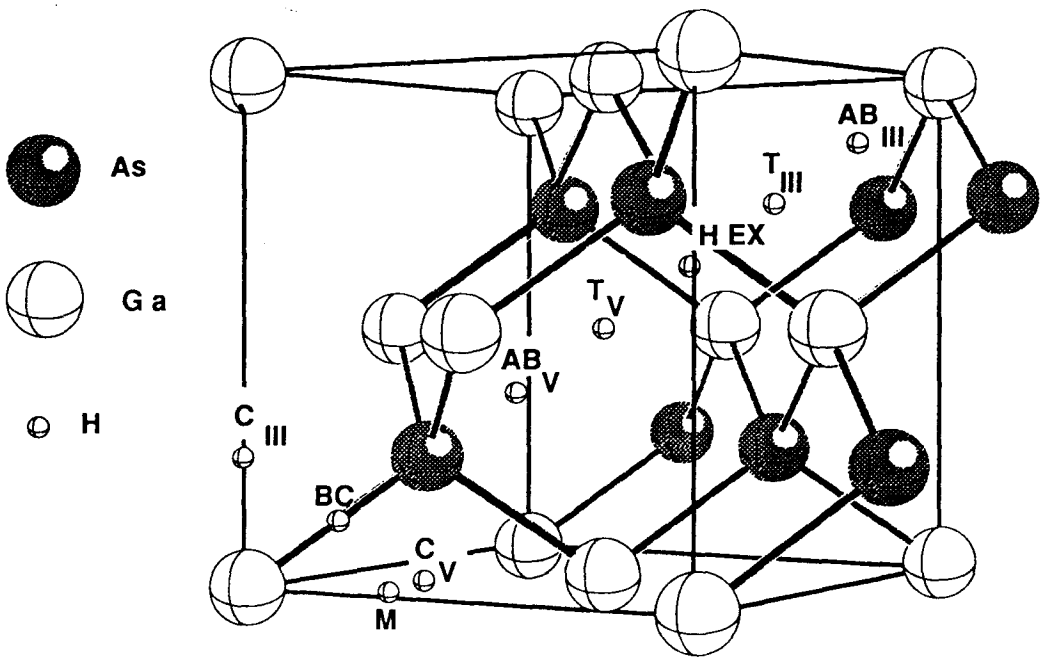

Figure 1-1. Tetrahedral (T_{III} and T_V), antibonding and bond centre sites for atomic hydrogen in crystalline GaAs (from L. Pavesi and P. Giannozzi[21])

(-0.83eV/kT) cm^2/sec. (Si E_a ~ 0.5 eV see Conyers et al). Zavada et al[25]. found from SIMS profiling measurements in the 200 - 600 °C range the diffusivity, D, to be D = 1.5×10^{-5} exp(-0.62 eV/kT) cm^2/sec in n-type GaAs.

The temperature range of interest (200 - 400 °C) is high enough such that atomic hydrogen diffuses into the bulk GaAs readily[26].

Hsieh et al[27]. found dislocations can provide pathways for atomic hydrogen diffusion, feeding hydrogen deep into the bulk.

In their study of buried n-type silicon doped GaAs layers grown by MBE deuterated at 220 °C Caglio and co-workers[28] found an increase in the room temperature electron mobility from 2270 cm^2/Vs (undeuterated) to 3950 cm^2/Vs accompanied by a reduced carrier concentration. Caglio and co-workers found the *diffusing* deuterium concentration was independent of layer doping level but the *bound* deuterium concentration in the doped layer was very close to that of its silicon concentration.

1.3.3 HYDROGEN PLATELETS IN GALLIUM ARSENIDE

Hydrogen platelets oriented along the {111} planes have been observed in proton bombarded GaAs during tunneling electron microscope studies[29].

It is believed from thermal effusion spectra that atomic deuterium forms complexes with lattice atoms and/or extended defects in bulk GaAs[30]. Deuterium incorporation stemmed from exposure of the GaAs to a remote dc D_2 plasma in the temperature range of 100 - 250 °C. An unexplained high temperature thermal effusion peak lead Stutzmann et al.[30] to believe extended defects may exist in the bulk of their deuterated sample.

1.3.4 H_2 ADSORPTION ON GALLIUM ARSENIDE

Molecular hydrogen can be considered a noninteractive, inert species with respect to surface reactions on GaAs in the temperature range of this study. Due to the fact that H_2 molecular orbital levels and As surface atom valence orbital levels are substantially different, H_2 and As orbital overlap can not occur, so H_2 does not stick to or dissociate on the (100) GaAs surface[31]. Other calculations have found the activation barrier for dissociative adsorption of molecular hydrogen to be ~ 2.5 eV[32].

1.3.5 ATOMIC HYDROGEN ETCHING GALLIUM ARSENIDE

Of the many steps in semiconductor device production between crystal growth and device testing this study focuses upon a processing essential known as *etching*. Etching is the removal of material (here crystalline GaAs) via some physical or chemical reaction. The rate of reaction of the etchant with the semiconductor as a function of temperature helps determine the feasibility of various processing techniques. Etching reactions relevant to semiconductors are between the gas or liquid phase etchant and the solid semiconductor. Reactions of atomic hydrogen with GaAs have been the subject of limited study through the exposure of GaAs to H <u>in</u> an H_2 radio frequency, microwave or Electron Cyclotron Resonance (ECR) plasma. To date there has been no study of the more fundamental reaction between GaAs and thermalised H. This etching reaction is not unambiguously known to occur.

Several published papers have appeared describing the cleaning of GaAs with hydrogen plasmas which yield useful information pertinent to the etching of GaAs. In general, it is found that atomic hydrogen from a plasma is effective at removing surface contamination such as carbon and oxygen compounds. Below

some of this work is summarized primarily focusing on the technique employing an ECR plasma leading to incident energies for the impinging neutrals on the order of 10 eV.

Hydrogen discharges were found in 1981 by Smolinsky, Chang and Mayer[33] not to etch GaAs or its oxide. Shortly thereafter Chang and Darack[34] first reported etching of both p- and n-type GaAs, and its oxides, with a hydrogen plasma establishing GaAs etch rates of 20 Å/min could be easily achieved. It was hypothesized the reactive species in the plasma, at least with respect to the oxides, was atomic hydrogen. The sample temperature was not estimated; however, the sample was within the discharge region . It was determined by the authors that the selectivity ratio of the oxide etch over the substrate was approximately two. Chang et al.[35] in a later publication eventually put an upper limit on the substrate temperature during etching in an H_2 plasma of 150 °C and described the resulting surface morphology and composition. Auger Electron Spectroscopy (AES) scans of the etched GaAs surfaces showed no elemental segregation whereas they did claim in the same paper that indium droplets formed on hydrogen plasma etched InP surfaces. A post-etch surface morphology comparison of Liquid Encapsulated Czochralsky (LEC) grown GaAs with that of Molecular Beam Epitaxy (MBE) grown GaAs convinced Chang et al.[35] that surface roughening is most likely a result of initial surface pits and defects on the LEC samples. The etched and unetched MBE samples were reported virtually indistinguishable, whereas the LEC grown samples were roughened during etching.

Okubora and co-workers[36] in 1986 reported what they considered to be molecular hydrogen etching of GaAs, under an AsH_3 overpressure, at temperatures in excess of 800 °C. Okubora and co-workers found no difference in etch rates between undoped and Si doped n-type GaAs. We propose that they were just etching the As and evaporating the Ga. They suggested the rate limiting step in

that reaction is the evaporation of gallium for they had obtained an activation energy, E_a=2.6 eV, in this temperature range nearly equal to the heat of evaporation of gallium. An activation energy approximately equal to the heat of evaporation of Ga is not surprising. The As removal has a very low activation energy so As desorbs easily. The decomposition of AsH_3 into H_2 and As_2 can, as they suggested, be regarded as being 100%. Then applying Le Chatelier's principle one can see that As from the surface may feed the reaction pushing it toward the formation of AsH_3 resulting in As removal. Gallium eventually evaporates and the process repeats. When Ar replaced the H_2 in the ambient gas mixture no etching was observed, suggesting the H_2 was indeed the "etchant" and that the As evaporation at this high temperature was minimal due to the AsH_3 overpressure. Okubora and co-workers also found, within the limits of AsH_3 partial pressure of 0.75-12 Torr, the GaAs etch rate with H_2 was independent of the AsH_3 pressure. The H_2 partial pressure was 300 Torr and 600 Torr in the two reported experiments in which the AsH_3 partial pressure was varied. Okubora and co-workers proposed the first step of the reaction kinetics involves chemisorption of atomic hydrogen, for the fraction of dissociated hydrogen should be at least $1x10^{-5}$ at 800 °C. This etching technique yielded "smooth... and mirrorlike" surfaces from their LEC grown undoped SI-GaAs samples. With an AsH_3 overpressure they could achieve congruent loss of Ga and As, but without it they observed Ga droplet formation.

In agreement with the earlier work of Chang and Darack[34], Sugata et al.[37] showed, in 1988, that Ga and As stoichiometry is maintained during cleaning with a hydrogen radical beam from an ECR plasma as determined by auger electron spectroscopy. Their radical beam consisted of mostly H^+ ions. This cleaning results in the reduction of the interface surface state concentration rendering it suitable for preparing samples for MBE pretreatment. Sugata et al. believe the rate limiting step to be the chemisorption rather than the desorption or reactant formation.

Reflection High Energy Electron Diffraction (RHEED) measurements suggested crystallinity was maintained and all cleaning was performed with the substrate temperature less than 400 °C.

K.C. Hsieh et al.[27] exposed thin Metallorganic Chemical Vapor Deposition (MOCVD) grown GaAs on a Si substrate to a hydrogen plasma but their etch rates (resulting in the removal of nearly all three microns of GaAs) could not be assumed to be uniform over time so no useful activation energy could be derived from this data. Hsieh et al. did however find the resulting surface after a two hour etch to be "pyramid-like," and after a five hour etch, in apparent contrast to the work of Chang and Darack[34] and Sugata et al.[37], metallic gallium "particles" were seen (via TEM microscopy) to form on the surface presumably due to prolonged exposure and utter consumption of the sample under investigation. To our knowledge this is the first report of Ga droplet formation on GaAs during a hydrogen atom etch. Previously, the droplet formation had only been reported during annealing[36] of GaAs where the As evaporation had left a Ga rich surface.

M-C. Chuang and J.W. Coburn[38] were the first to report the products formed *during* a hydrogen plasma etch of GaAs. They observed only volatile arsenic hydrides with mass spectrometry during exposure of GaAs to hydrogen atoms from a plasma in the presence of Ar ions, but claimed no products were formed in the presence of hydrogen atoms without simultaneous argon ion bombardment (i.e. hydrogen atoms alone appeared to not react with GaAs). They observed neither gallium hydride species with the mass spectrometer nor gallium droplet formation. AES performed on the resulting surface indicated an increased As deficiency. This enigma is still far from resolution since Chuang and Coburn observed no GaH_x despite the fact that hydrogen plasmas are well known to etch GaAs.

I. Suemune and co-workers[39] next found the hydrogen atom etch rate of GaAs decreased with increasing angle of incidence (from the substrate normal) of

their hydrogen ECR plasma beam and their etching even ceased after reaching a depth of 20 Å for shallow incident angles apparently leaving an atomically flat (100) surface. The etch rates they (Suemune co-workers) found were approximately a factor of 100 slower than our measured etch rates with the difference merely assumed to be attributed to vastly different hydrogen atom concentrations.

J.R. Creighton[40] exposed (100) GaAs at 150 K to hydrogen atoms created by dissociation of H_2 on a hot tungsten filament. Temperature Programmed Desorption (TPD) studies were carried out and again (as in reference 38) no gallium-hydrides were observed. Creighton attributed the elusiveness of gallium-hydrides to surface hydride decomposition resulting in molecular hydrogen formation.

By using a hot tungsten foil in the presence of H_2, J.A. Schaefer et al.[41] exposed GaAs to H atoms and subsequently identified, via High Resolution Electron Energy Loss Spectroscopy (HREELS) studies, the formation and decomposition on the surface of both arsenic and gallium hydrides. This study; however, demonstrated the resulting surfaces were gallium rich. J.A. Schaefer and co-workers[42] later obtained results indicating increased hydrogen exposure leads to increased arsenic- and gallium-hydride formation (GaH and GaH_2) on the surface until the exposure was too high leading to gallium droplet formation.

During their *in-situ* RHEED monitoring of the same cleaning process as Kishimoto and co-workers[43] measured the etch rate of (100) GaAs at three substrate temperatures between 300 - 500 °C. Their etch rate data corresponds to an activation energy of 0.2 eV. The technique for the determination of their etch rate was not stated.

Another piece of information gleaned from a hydrogen plasma cleaning of GaAs publication is the formation of the stable Ga_2O_3 at temperatures less than 150 °C [44]. Mikhailov et al.[44] found through X-ray Photoelectron Spectroscopy (XPS) studies that this oxide may well be responsible for the inhibition of etches at

temperatures less than 150 °C. However they proposed that the decomposition of Ga_2O_3 and 2H yielding desorbed Ga_2O and water at higher temperatures can result in the removal of the oxide.

SECTION 2: EXPERIMENTAL

2.1 REACTION VESSEL

GaAs was exposed to large fluxes (~ 5 mTorr) of atomic hydrogen downstream from a low pressure (0.4 Torr) H_2 plasma resulting in a chemical reaction between the gas phase H atoms and the solid phase GaAs. The reactor, including valve bodies, was entirely Pyrex (see Figure 2-1). This "fast" flow system was driven with a Welch Duo-Seal model 1402 45 l/min (at 0.5 Torr) rotary pump which provided an H_2 flow from a standard cylinder of 40 sccm over the sample. The pressure in the flow system is measured with an Edwards capacitance type manometer. A microwave discharge was created 15 cm upstream from the sample. The sample temperature was measured by a thermocouple mounted within the sample holder.

The reaction tube was 20 mm in diameter in the region of the gas - solid reaction. Since the reaction was found to only proceed above 180° C, the walls of the reactor and hence the gas and sample were heated by wrapping a heating tape around the outside of the reactor leaving as small an apperture as possible in order to permit the passage of the incident and reflected laser light neccesary to monitor the etch *in-situ*. The heater "tape" was across the output of a Variac. Adjusting the ac voltage output of the Variac controls the power the heater "tape" delivers to the reactor and hence the reactor, sample and gas temperature. It is presumed the walls, sample and gas are in thermal equilibrium under any given etchant gas flow conditions.

The room temperature gases, carried by copper tubing, that were admitted into the flow system through needle valves were prepurified H_2 and N_2 supplied by Linde and according to supplier's specifications were 99.99 and 99.998 % pure respectively. The H_2 flow rate was measured with a Sierra Top-Track mass flow

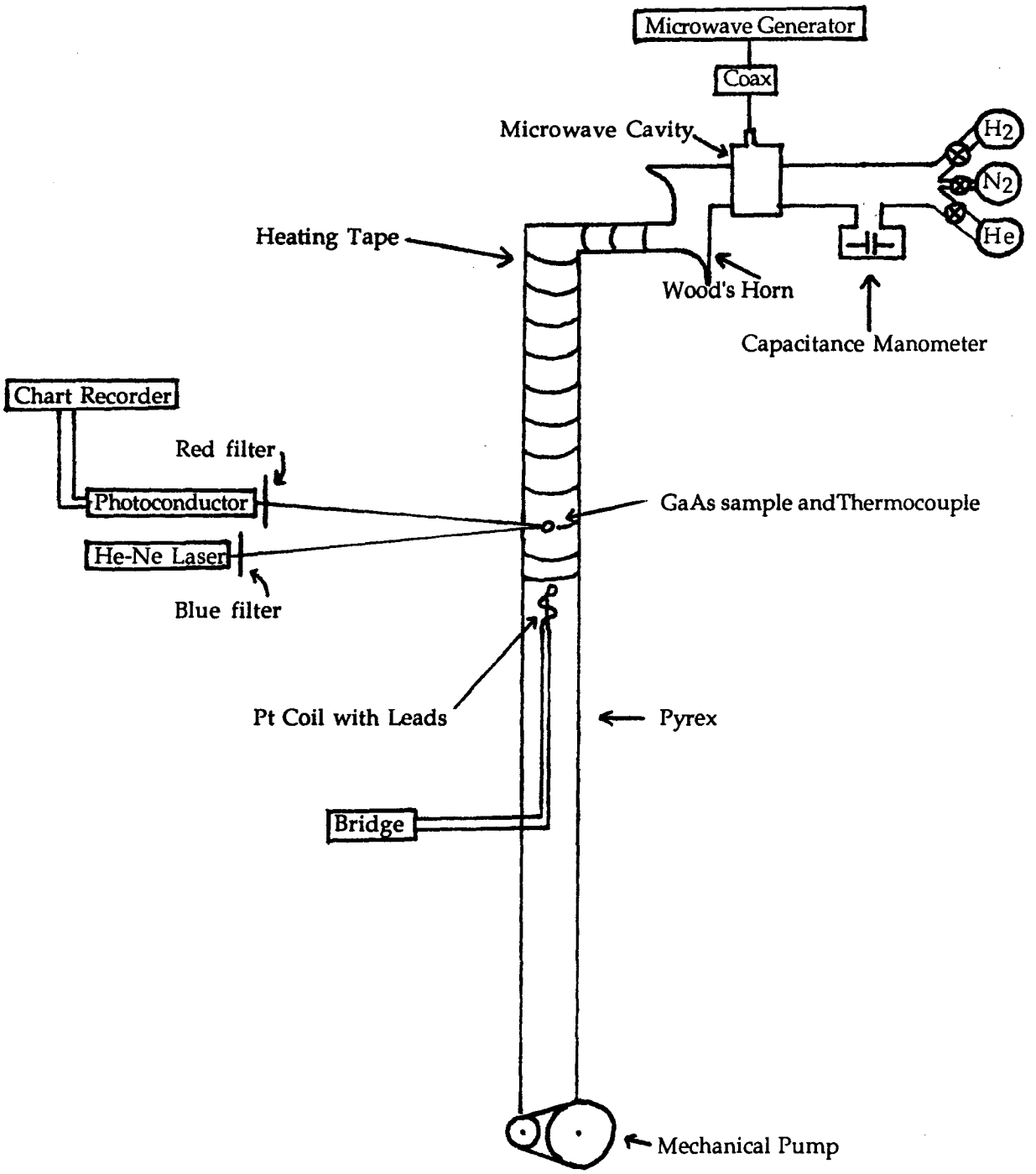

Figure 2-1. Schematic layout of flow system for H atom generation, detection and etching of (100) GaAs

meter. The N_2 flow rate was determined relative to the H_2 flow. To estimate the N_2 flow the flow of H_2 was remeasured by feeding the output voltage of the pressure guage to a chart recorder while bleeding the H_2 gas into the sealed reactor and recording the increase of pressure with time. The slope (=dP/dt) of the resulting plot is proportional to the flow of H_2. After pumping out the H_2 and repeating, the same prodedure is carried out flowing only N_2 gas. During an experimental run, the smaller N_2 flow is mixed with the larger H_2 flow. The high pressure side of the N_2 needle valve is ~ 1 atm overpressure, so the difference between the flow of N_2 in the absence of H_2 and in the presence of less than 1 Torr of H_2 is negligible. The resulting slope for the N_2 dP/dt tests was consistently ~ 10^{-3} of the H_2 slope. This indicates N_2 was ~ 0.1% of the total flow. This fraction was not particularly intended. It was merely the smallest measureable nonzero flow that could be obtained from the needle valve used to admit the N_2.

Care was taken to preserve gas purity during regulator installation by leaving regulator valves open during initial opening of the gas cylinder valves.

The H_2 gaseous flow in these experiments is on the order of 40 sccm and total pressures were just above 400 mTorr.

Vibration isolation is not elaborate in this experimental arrangement. A flexible rubber hose coupling the low pressure side of the vacuum pump to the reaction vessel is the only hint of vibration isolation. The etching of GaAs is followed *in-situ* by observing interference fringes produced by reflections off of the sample of visible red laser light which traverses a total path length of about one metre. The reflected laser light impinges on a photoconductor changing its electrical conductivity. This photoconductor is one element of a voltage divider. The dc voltage appearing across the constant resistance element of the voltage divider is fed to the input of a chart recorder. The periodicity of the interferogram (on the order of one hour) is much larger than that of conceivable vibrations from

the building or the system vacuum pump. However, vibratory motion of the sample holder will move the specular reflection off the sample such that it partially or completely misses the photoconductor. Clearly this can lead to fluctuations in the intensity of detected light which could be miscontrued as the manifestation of surface roughening. The two sample surfaces responsible for the laser reflection, the silicon nitride mask and the GaAs surface being etched, do not move relative to one another in the absence of etching (or growth) when the temperature of the sample is constant in time. Since the reflections from these surfaces are assumed solely responsible for the interference, the sample can undergo limited displacements without adversely affecting the resulting interferogram. Provided the specular reflection does not miss the photoconductor, vibratory motion of the sample holder and the sample does not result in substantial photoconductor voltage swings. Therefore, small variations of the sample holder about its equilibrium position result in no noticeable intensity flucuations.

Indeed, the Pyrex sample holder's thinness did lead to erroneous fluctuations in the detected light intensity which were correlated with sample and holder temperature variations. If the temperature is raised from 300 °C to 325 °C for example, the Pyrex sample holder may move due to thermal stress. The displacement associated with this could result in a total loss of the specular beam for the room temperature detector has not experienced a complimentary displacement. Some samples were etched at two temperatures. Data acquisition requiring a range of temperatures necessitated readjustment of system optics for each temperature and confidence thermal equilibrium has been established. Celophane tape was used to scatter the light incident on the photoconductor in an effort to reduce the detector's directionality making it less vulnerable to intensity shifts due to sample holder displacements.

To minimize noise from ambient light sources a red narrow pass filter was used (see Figure 2-1 for placement) resulting in the selection of primarily the neighboring wavelengths around the lasing transistion wavelength at 632.8 nm. A blue filter was also used to avoid saturation of the photoconductor.

2.2 SAMPLE HOLDER AND THERMOMETRY

The functionality of the sample holder draws on its ability to keep the sample in a fixed position, conduct heat away from the sample, allow interaction of the sample with the etchant, H, permit the measurement of the sample temperature and allow quick loading of the sample into the reactor. Sample holders were blown from 4" straight sections of 0.25 " OD Pyrex tubing (see Figure 2-2). The first step of sample holder fabrication is to close the tube at one end, then blow, stretch and flatten the glass under flame such that the wall thickness at this end of the tube is less than 0.1mm. A small area on this end of the sample holder is heated locally and a 180° bend is created resulting in a spring-like configuration. This spring depresses the GaAs sample against the aforementioned thin-walled section of the Pyrex tube. Within this tube, not in direct contact with the sample or the etchant gas flow, is a point contact Chromel Alumel J-type thermocouple connected to a Fluke readout displaying the sample temperature to the nearest 0.1° C. Confidence in the absolute sample temperature estimate is based largely on the fact that independent measurements of the temperature dependence of this reaction, made in this laboratory[45] with the thermocouple in direct contact with the sample yielded consistent results. Hydrogen atoms recombining to form H_2 on the thermocouple itself eliminate the possibility of direct exposure of the thermocouple to the hydrogen atom flow.

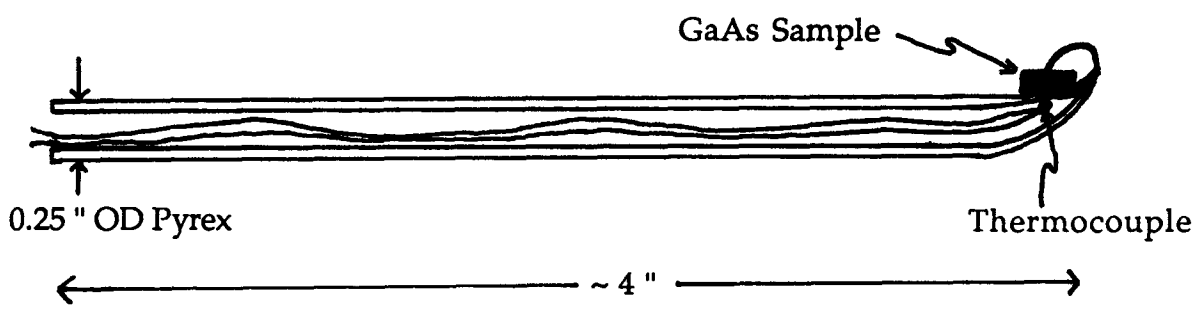

Figure 2-2. 0.25 " OD pyrex tubing sample holder with GaAs sample and thermocouple

2.3 GALLIUM ARSENIDE SAMPLES AND SILICON NITRIDE MASK

Undoped, semi-insulating single crystal LEC GaAs was grown by Johnson Matthey. The wafer was 2" diameter 0.5 mm thick mechanical grade (100) GaAs oriented 2° off axis. In order to follow the etching reaction, it was neccesary to pattern the wafer with an array of thin stripes which essentially transform the flat GaAs surface into a multislit optical interference device (see Figure 2-3). The mask used in this process consisted of two orthogonal 1 cm^2 areas of 15 μm wide straight lines separated by a distance of 15 μm. Several 2 cm^2 pieces were cleaved from the wafer and patterned seperately. This was achieved by firstly depositing a 950 Å silcon nitride film on our wafer. Then, half the silicon nitride was removed during this preparatory treatment through standard photolithography and etching techniques[45] resulting in 50% of the surface covered with nonreactive silicon nitride stripes. The processed wafer had silicon nitride (Si_3N_4) stripes 15 μm wide and 15 μm apart aligned on half of the total wafer area parallel to the <011> direction and on the other half perpendicular to it. Rectangular GaAs chips were cleaved from these 2 cm^2 pieces resulting in sample surfaces of ~ 0.2 cm^2 and sample volumes of ~ 0.01 cm^3. Other details of the nitride preparation can be found in the above reference.

Just prior to each experiment, the masked and cleaved (100) GaAs samples were immersed in a few millilitres of room temperature concentrated hydrochloric acid for about a minute to remove any native oxide layer. The samples then experienced an agitated dip in distilled water.

Before acquiring data, the samples were loaded onto the sample holder by slipping them under the glass spring in an N_2 ambient. Then the holder with sample is inserted into the heated, He back-filled reactor toward the center of flow.

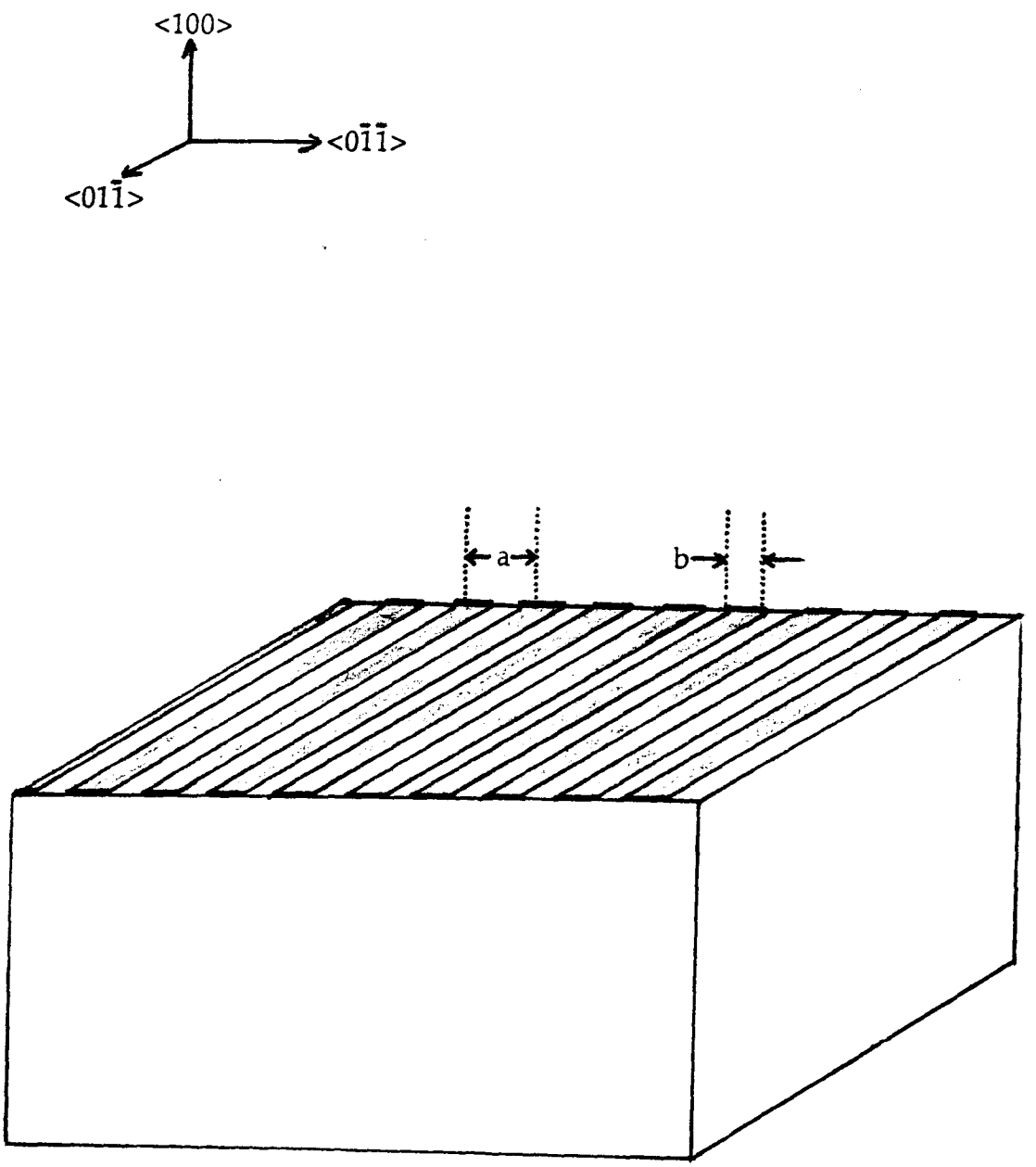

Figure 2-3. (100) GaAs with equally spaced silicon nitride stripes (a = 30 μm, b = 15 μm). Mask alignment along each the <01$\bar{1}$> and <0$\bar{1}\bar{1}$> were used.

2.4 HYDROGEN ATOM PRODUCTION

Atomic hydrogen is obtained by dissociation of molecular hydrogen. This is achieved by passing a short length of the reactor (cross sectional area ~ 1 cm^2) with its flowing H_2/N_2 gas mixture (H_2 and N_2 are mixed several centimeters upstreamfrom the discharge) through a coaxial cable fed quarter wave microwave cavity with 50 W at 2.45 GHz (λ = 12.2 cm) incident upon it from an E.M.I. *Microtron 200* microwave power generator. The cavity is equipped with a port for cooling air which provides for heat removal from the hot walls containing the resulting plasma.

No "wall poisons" are employed in the present configuration of this apparatus. Wall poisons such as phosphoric acid are often intentionally used to increase the hydrogen atom concentration[46] for the products that can be withdrawn from a pure H_2 plasma in a clean pyrex tube contain very few H atoms. The reaction rates which we investigate in this experiment commonly necessitate constant hydrogen atom concentrations over periods of one to three hours. The decay in time of the effectiveness of these "poisons" lead the author to try other means of sustaining a constant concentration. Certainly, a constant and generous supply of H is required for a kinetic study of this kind.

An alternative to wall poisons is to "trickle" pre-purified nitrogen gas into the predischarge flow of H_2. Similarly, other researchers have added trace amounts, 0.1 - 0.3 %[47], of H_2O or O_2 to reduce recombination of H in H_2 plasmas. This provides the long term stability necessary for these protracted reaction rate measurements. Purified H_2 gas flows through the reactor with 0.1 % purified N_2 added to stabilize the hydrogen atom concentration over periods of several hours. Larger flows of nitrogen were found to substantially retard the etch rate.

2.5 HYDROGEN ATOM DETECTION

The hydrogen atom concentration was determined with an isothermal calorimetric probe[48] which uses the heat of recombination of the atoms on a platinum wire to measure the hydrogen atom flow. A comparison of the absolute H concentration determined via the platinum wire with that determined via a H + NOCl titration found agreement within 1 %[49] . A 15 cm length of platinum wire (AWG #30) was coiled to occupy as much of the reactor's flow cross-section as possible (as in Figure 2-4). The biased coil (and its leads) behaves as a resistive branch of a Wheatstone bridge configured in a 1 : 1 ratio (see Figure 2-5).

A ten turn potentiometer adjusts the current and another ten turn potentiometer adjusts the opposite variable branch of the bridge. A digital voltmeter is the null detector measuring the "null" voltage to the nearest 100 μV.

The isothermal calorimeter is comparable to that of E.L. Tollefson and D.J. LeRoy in their pioneering experiments of hydrogen with acetylene[48] The platinum wire was wound and spot welded to two stainless steel lead-in rods 3 mm in diameter. The vacuum seals between the glass and rods are made of ***Torr Seal*** ® epoxy. The stainless steel rods are exposed to the hydrogen flow with no adverse effects upon the quantitative hydrogen atom concentration for they are downstream from the detector, where all the atoms have been removed.

The purpose of the bridge is to monitor as accurately as possible the temperature dependent dc resistance of the Pt wire. Keeping the detector in equilibrium with the walls of the reaction tube is the "name of the game" for the isothermal calorimeter. What it does best is utilize the Wheatstone bridge to measure changes in the resistance of the wire corresponding to temperature changes in the wire. The hydrogen atoms available for the reaction under investigation recombine on the Pt wire to form hydrogen molecules. The heat of recombination of the hydrogen atoms tends to warm the Pt wire increasing its dc

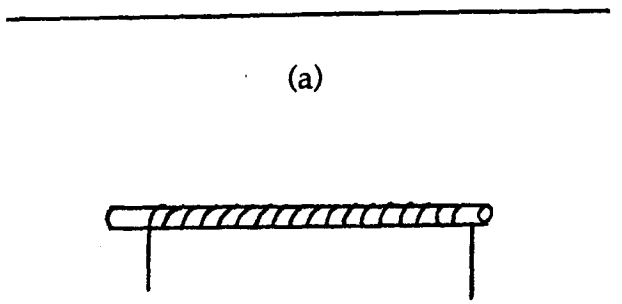

(a)

(b)

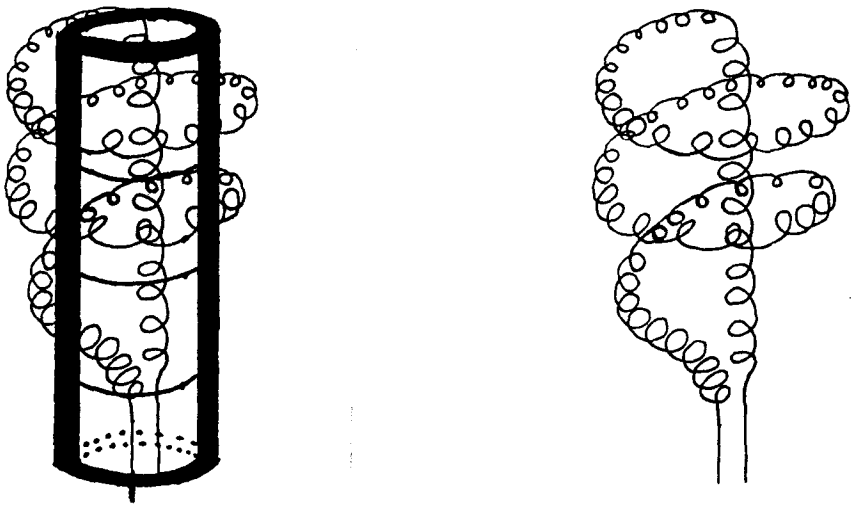

(a) (d)

Figure 2-4. Winding process for Pt wire H atom detector (a) straight AWG #30 Pt wire, (b) wind Pt wire around 0.125 " OD glass tubing, (c) use 0.4 " glass tube as a form to shape Pt wire into spiral from already coiled wire, (d) final Pt wire configuration, as in the reactor

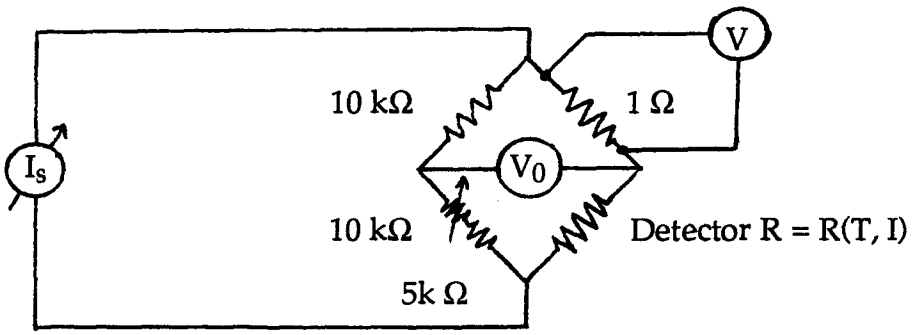

Figure 2-5. 1 : 1 Wheatstone bridge configuration for H atom detection with current regulator, I_s, null detector voltmeter, V_0, Pt wire detector, R, and voltmeter, V, to imply coil current

resistance and destroying the sensitive balance of the bridge. Immediate decrease of the bridge current upon ignition of the discharge from its initial value I_{off} to some final value I_{on} where I_{off} (> I_{on}) rebalances the bridge due to the resulting restoration of its temperature and resistance.

An actual experimental determination of the hydrogen atom concentration in the flow system consists of a measurement of I_{on} with the H_2/N_2 discharge on in the steady state (i.e. $dT/dt = 0$) followed by a measurement of I_{off} with the discharge extinguished. The thermal conductivity of the flowing gas remains constant regardless of the status of the discharge. Only H_2 should be carrying heat away from the Pt wire. Since the dissociation of H_2 in the region of interest of this experiment (downstream from the discharge) doesn't exceed 3% (see Section 3) the Pt wire's thermal link to the walls of the reaction vessel, remains constant, eliminating perturbations to thermal equilibrium due to discharge status dependent variations in the thermal conductivity between the detector wire and the vessel wall.

Knowing one experimental parameter other than the difference in coil current with the discharge off and on, namely the dc resistance of the Pt wire at its operating temperature, an absolute determination of the heat added to the Pt wire per second and hence the total heat of recombination per second can be found from the relation between power, current and resistance:

$$P = \Delta(I^2) \times R_{Pt}$$

where $\Delta(I^2) = I_{off}^2 - I_{on}^2$ and R_{Pt} = Pt wire dc resistance. This heat per second added to the wire has been shown to be[49] directly proportional to the absolute number of hydrogen atoms per second (assuming the detector's efficiency is unity) in the reactor's flow. If one divides P by the heat given off by the exothermic

recombination reaction of $H+H \rightarrow H_2$ (218 kJ/mol of H) one is left with the number of moles of atomic hydrogen per second:

$$\text{H atom flow [mol/sec]} = \frac{P\,[\text{J/sec}]}{218\ \text{kJ/mol}}$$

To calculate P_H we can use the measured H atom flow, H_2 flow and total reactor pressure,

$$P_H = \frac{\text{H atom flow [mol/sec]}}{H_2\ \text{flow [mol/sec]}} \times \text{total pressure}$$

where the mol/sec of H_2 are found simply by multiplying the flow of H_2 from the flow meter by its density . The STP molar volume of H_2 can be used in this calculation to determine the flow of H_2 in moles per second because the H_2 source flow is measured in standard cubic centimeters per minute (sccm).

$$\text{STP Molar volume of } H_2 = 22.43\ \text{l/mol} = 2.243 \times 10^4\ \text{cm}^3/\text{mol}$$

$$\text{Density of } H_2 = 1/\text{molar volume} = 4.458 \times 10^{-5}\ \text{mol/cm}^3$$

$$\text{mol/sec of } H_2 = \frac{\#\text{sccm of } H_2 \times 4.458 \times 10^{-5}\ \text{mol/cm}^3}{60\ \text{sec/min}}$$

The H_2 flows in this study, on the order of 40 sccm, correspond to approximately 3×10^{-5} mol/sec.

2.6 INTERFEROMETER

The probe for material removal observation is a 10 mW 632.8 nm He-Ne laser operating in continuous mode and shone upon the effective multislit

aperture created by the sample's silicon nitride stripes (as in Figure 2-3). The receding surface from which material is removed reflects part of the beam of photons from the laser while the silicon nitride, unaffected by the hydrogen atom etchant, reflects the remaining fraction of the beam. In the limit of a perfectly constant etch rate this configuration is a small scale Lamellar Grating Interferometer. Invented in the 1950's by Strong and Vanasse at Johns Hopkins University[50], the full scale version is more commonly used in Fourier Transform Spectroscopy.

Unlike reflected photons from the silicon nitride, those from the GaAs experience a rather continuous change in optical path length. Etching of the GaAs leads to an oscillation in the reflected light intensity at a point far from the sample. The periodicity of this oscillation can be predicted by the relation

$$\frac{n\lambda}{\eta} = 2d\sin\theta\Big|_{\theta=\pi/2}$$

where η is the refractive index of air at 632.8 nm (assumed unity) and θ is the angle of incidence relative to the (100) GaAs surface and $d\sin\theta$ is the added optical path length a photon reflected off the GaAs surface experiences relative to a photon reflected off the silicon nitride. Due to the fact that the detector and light source can not occupy the same place in space, there is some error associated with the approximation that $\theta = \pi/2$. With our detector and light source geometry (one on top of the other) the angle of incidence is closer to $\pi/2$ - 0.035 rad (88 °) which results in less than a 0.2 % error in $\sin\theta$.

Constructive interference of the beams reflected off the different surfaces will occur for the zeroth order reflection whenever $2d = n\lambda$, or equivalently, anytime the depth of the etch is a multiple of $\lambda/2$.

A light intensity dependent voltage from a biased silicon photoconductor is sent to a chart recorder which simply plots the intensity of the reflected specular

beam from the sample versus time (see Figure 2-6). The resulting interferogram has a periodicity corresponding to half of the He-Ne's wavelength (i.e. two cycles of the interferrogram depict the removal of approximately 633 nm of material from the GaAs surface). The geometry of the silicon nitride stripes turns out to be of some consequence to the signal-to-noise ratio of the interferometer. One simple silicon nitride step is sufficient to give interference as described above. However, experimentors in this laboratory have found the smallest stripe width, b, and the smallest center to center stripe separation, a, yields the most discernible interferogram on the chart recorder paper.

When the He-Ne laser is shone onto the striped sample, the reflected light intensity has the same angular dependence as a diffraction grating. When light is incident normal to a diffraction grating the first (not zeroth) principal maximum occurs at an angle (measured from the surface normal), θ_1, where θ_1 satisfies

$$a\sin\theta_1 = 1\lambda,$$

where a is defined as above and λ is the He-Ne wavelength (632.8 nm). So θ_1 depends on a and λ via,

$$\theta_1 = \sin^{-1}(\lambda/a).$$

This angular separation of the zeroth and first principal maxima in the diffraction pattern corresponds to a separation in space, Δs, at the detector (~0.5 m from the surface)

$$\Delta s = r \times \theta = 0.5\ \mathrm{m} \times \theta_1.$$

Silicon nitride stripes on (100) GaAs from 15 μm widths (=b) separated by 15 μm (=a/2) to 100 μm widths separated by 100 μm have been used in this laboratory. Evaluating θ_1 (i.e. the angular separation between the zeroth and first principal maxima) using the above expression and these two values of a,

$$\theta_1(a=30\mu\mathrm{m}) = \sin^{-1}\left(\frac{632.8 \times 10^{-9}\ \mathrm{m}}{30 \times 10^{-6}\ \mathrm{m}}\right) = 2.1\times10^{-2}\ \mathrm{rad}\ \ [15\ \mu\mathrm{m}\ \mathrm{stripes}]$$

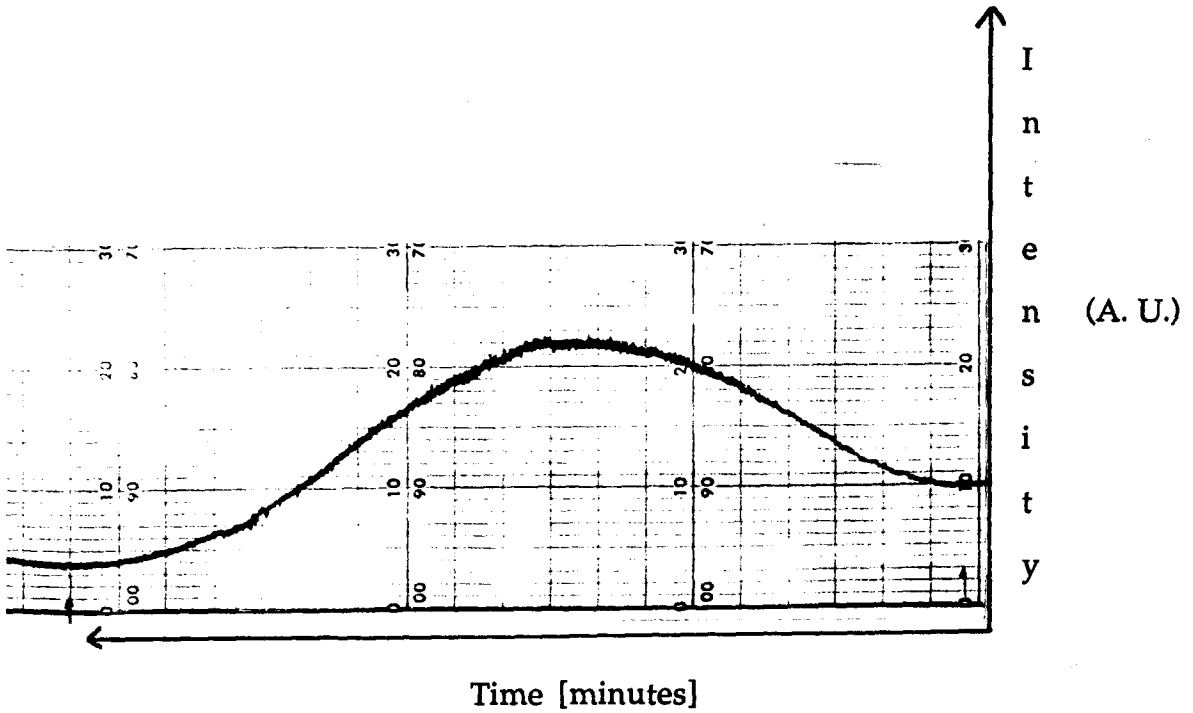

1 division = 5 minutes

Figure 2-6. Photoconductor's output as a function of time. One 1.5 hour period, corresponding to H atom etching of 316 nm of (100) GaAs at 281 °C.

$$\theta_1(a=200\mu m) = \sin^{-1}\left(\frac{632.8 \times 10^{-9}\ m}{200 \times 10^{-6}\ m}\right) = 3.2\times10^{-3}\ \text{rad}\ \ [100\ \mu m\ \text{stripes}].$$

These angular separations lead to a spatial separation, Δs, between the zeroth and first principal maxima at the detector (0.5 m away),

$$\Delta s = 0.5\ m \times 2.1\times10^{-2}\ \text{rad} = 1.1\ cm\ \ [15\ \mu m\ \text{stripes}]$$

$$\Delta s = 0.5\ m \times 3.2\times10^{-3}\ \text{rad} = 1.6\ mm\ \ [100\ \mu m\ \text{stripes}].$$

With the He-Ne laser light close to normal incidence in the presence of etching, all the diffraction orders[51] are modulated, due to the aforementioned phase difference, by an <u>order dependent</u> $\cos^2\delta$ term, i.e. the angle dependent intensity is:

$$I(\theta) = \frac{I(0)}{N^2}\,\text{sinc}^2\beta\left[\frac{\sin N\alpha}{\sin\alpha}\right]^2 \cos^2\delta$$

where $\beta \equiv \frac{\pi b}{\lambda}\sin\theta$ and $\alpha \equiv \frac{\pi a}{\lambda}\sin\theta$ and θ, a, b and λ are defined as above.

So,

$$I(\theta) \propto \cos^2\delta$$

where δ is given by,[52]

$$\delta = \frac{\pi m}{2} + \frac{2\pi d}{\lambda}$$

where m is the order of interest, λ is the He-Ne wavelength and d (a function of time) is the difference in height between the silicon nitride and the GaAs. Due to the form of the δ order dependence, the intensity oscillations of the zeroth and first order are π out of phase with respect to each other (see Figure 2-7). This can be seen by examining δ for both the zeroth and first order (i.e. m=0, ±1) evaluated also at the height differences corresponding to both constructive ($d=\lambda/2$) and destructive ($d=\lambda/4$) interference for the zeroth order.

$$\delta(m=0, d=\lambda/2) = \pi;\ \cos^2\delta = 1$$

$$\delta(m=\pm1, d=\lambda/2) = \pm\pi/2;\ \cos^2\delta = 0$$

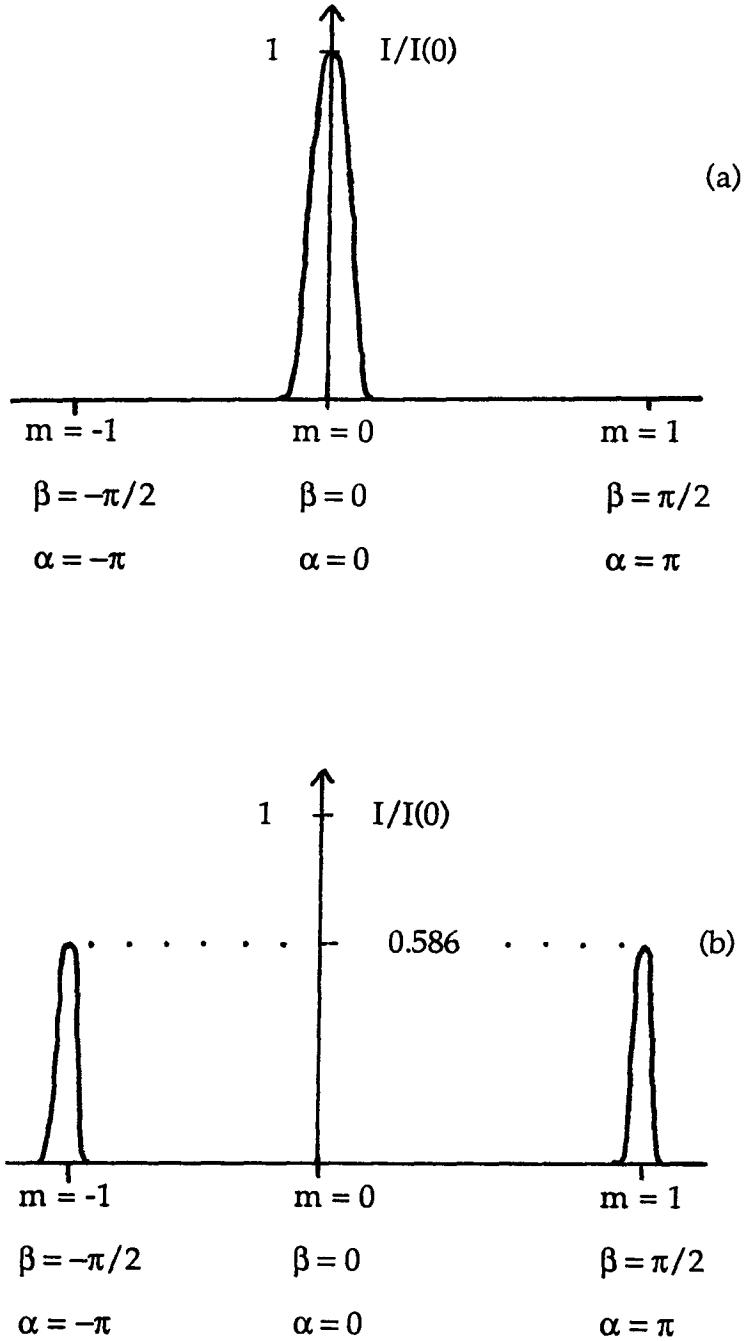

Figure 2-7. Angular dependence of irradiance from a Lamellar Grating Interferometer with a = 2b at an etch depth, d, of (a) $\lambda/2$ and (b) $\lambda/4$

$$\delta(m=0, d=\lambda/4) = \pi/2; \cos^2\delta = 0$$

$$\delta(m=\pm1, d=\lambda/4) = 0, \pi; \cos^2\delta = 1$$

Since the intensity is proportioal to $\cos^2\delta$ one can see that constructive interference in the zeroth order coincides with destructive interference in the first order (the converse is also true).

It is found upon substitution of the above values of $\cos^2\delta$ into the intensity expression and setting a = 2b that,

$$I(m=0, d=\lambda/2) = I(0)$$

$$I(m=0, d=\lambda/4) = 0$$

$$I(m=\pm1, d=\lambda/2) = 0$$

$$I(m=\pm1, d=\lambda/4) = 0.586\ I(0)$$

This phase dependent modulation of the orders neccesitates spatial separation of the orders if one desires to observe maximum modulation of the reflected light amplitude. It is apparent from the above calculation that the zeroth order maximum and the first (actually all odd) order maxima vary sinusoidally in relative phase as well as in amplitude as the etch progresses. If, neglecting contributions from higher orders, both zeroth and first orders are "seen" by the photoconductor (i.e. the orders nearly overlap in space), in this case of 15 μm silicon nitride stripes, the light intensity will be the sum of the two "out of phase" beams which leaves

$$I_{net} = [2 \times 0.586 - 1]\ I(0)$$

where one factor of 0.586 comes from each of the m=±1 orders

$$I_{net} = 0.17\ I(0).$$

Whereas if the zeroth order only is "seen" by the phototconductor a total swing in light intensity equal to I(0) is possible. Therefore, best results are obtained when the zeroth order maximum can be separated from the others.

Since our detector diameter is of the order 5 mm, it is clear that the 15 μm striped samples (Δs = 1.1 cm) would lead to an enhanced signal to noise ratio over that of the 100 μm striped samples (Δs = 1.6 mm) since the zeroth order maximum from the 15 μm striped sample alone will be incident upon the detector.

A blue filter was used to prevent saturation of the phoconductor from the He-Ne's specular reflection off of the GaAs and to minimise the laser enhancement of the etching. A simple transmission experiment was performed to determine the extent to which the filter attenuated the light. At the wavelength of interest, 632.8 nm, the filter was found to reduce the laser's intensity 23%. Also of relevance is the attenuation of the light from a single pass through Pyrex into the reactor. The transmission coefficient for pyrex at 630 nm is ~ 0.9. The sum of the attenuations is ~33%, hence the power of the laser light incident on the GaAs is about 6.7 mW, corresponding to 2×10^{17} photons/sec.

The etching reaction yielded such textured surfaces that a fraction of the reflected light that makes it to the detector could conceivably come from subsurface reflections of the incident light from extended defects or other related abrupt refractive index changes. Owing to the different index of refraction for GaAs relative to air, a single interference fringe resulting from superposition of a subsurface reflection with a surface reflection would then correspond to removal of less material then would be expected under the assumption the two interfering waves are of the same wavelength (632.8 nm). The possibility of sytematic error in the etch depths, and hence the etch rates, was eliminated by comparison of the interferometry etch depth measurements with post-etch depth measurements made with both a scanning electron microscope and a Tencor Alpha Step 200 profilometer.

SECTION 3: RESULTS

3.1 MEASUREMENT OF THE ATOMIC HYDROGEN CONCENTRATION

A determination of the rate constants for the H atom etching of (100) GaAs is only possible when the reaction (etch) rate as well as the absolute hydrogen atom concentration are known. The atomic hydrogen partial pressures were measured just below the GaAs samples downstream from the microwave H_2 discharge. The reactor pressure was on the order of 400 mTorr (1 - 2 % atomic H) and hydrogen atom partial pressures were measured in the 200 - 360 °C range.

The rate at which *heat* is added, P, to the platinum wire *from H atom recombination* is obtained from the product of the platinum wire's electrical resistance at its operating temperature and the difference of the squares of the platinum wire's current neccesary to maintain a constant temperature in the presence (I_{on}) and absence (I_{off}) of H atoms. While etching at 360 °C, for example, the power the atoms contributed to the platinum wire was,

$$P = 0.0420\ A^2 \times 2.06\ \Omega = 86.4\ \text{mW}.$$

The measured H_2 flow rate, along with the STP density of H_2 gas and the known energy released in H recombination (217.9 kJ/mol), now permits the computation of the partial pressure of atomic hydrogen.

$$H_2 \text{ flow} = 42 \text{ sccm}$$

$$\text{total pressure} = 0.431 \text{ Torr}$$

$$P_H = \frac{0.0864\ \text{W} / 218 \times 10^3\ \text{J/mol}}{42\ \text{sccm} \times 4.458 \times 10^{-5}\ \text{mol/cm}^3} \times 60\ \text{sec/min} \times 0.431\ \text{Torr}$$

These values lead to a hydrogen atom partial pressure, P_H

$$P_H = 5.46 \text{ mTorr.}$$

The measured hydrogen atom concentrations in this study varied from 3 - 10 mTorr (see Table 3-3 below).

3.2 MEASUREMENT OF THE ORDER OF THE REACTION WITH RESPECT TO THE CONCENTRATION OF ATOMIC HYDROGEN

From a compilation of the author's acquired data and independently acquired data of another experimentor in this laboratory[43] (Tables 3-1 and 3-2) two estimates of the order of the reaction of the (100) GaAs surface with respect to the hydrogen atom concentration are made. The order can only be tested by experiment. One needs to etch at one temperature over a range of etchant concentrations. The etch rate at a given temperature, r, in general should be proportional to the H atom concentration to some power, x, i.e.

$$r = k[P_H]^x$$

where x is the order of the reaction which can take on positive or negative fractional or integer values or even zero. A plot of the natural log of the etch rate at some temperature vs. the natural log of the partial pressure of H atoms yields a slope *equal* to the order of the reaction with respect to atomic hydrogen.

$$\ln r = x\ln [P_H] + \ln k$$

Figure 3-1a and Figure 3-1b are plots of the log - log data in Tables 3-1 and 3-2. The slopes are found to be 0.90±0.06 and 0.8±0.1 at 250 °C and 280 °C, respectively

Table 3-1

Etch Rate, r (nm/min)	H Partial Pressure (mTorr)	ln r	ln P_H
3.20	4.68	1.16	-5.37
4.52	7.74	1.51	-4.86
26.4	51.0	3.273	-2.98

Table 3-2

Etch Rate, r (nm/min)	H Partial Pressure (mTorr)	ln r	ln P_H
5.70	4.72	1.74	-5.36
3.37	3.27	1.22	-5.72
15.1	2.66	2.72	-3.63
21.7	26.7	3.08	-3.62

Tabulated data for estimation of the order, x, of the GaAs etching reaction with respect to the atomic hydrogen concentration, P_H at 250 °C (Table 3-1) and 280 °C (Table 3-2).

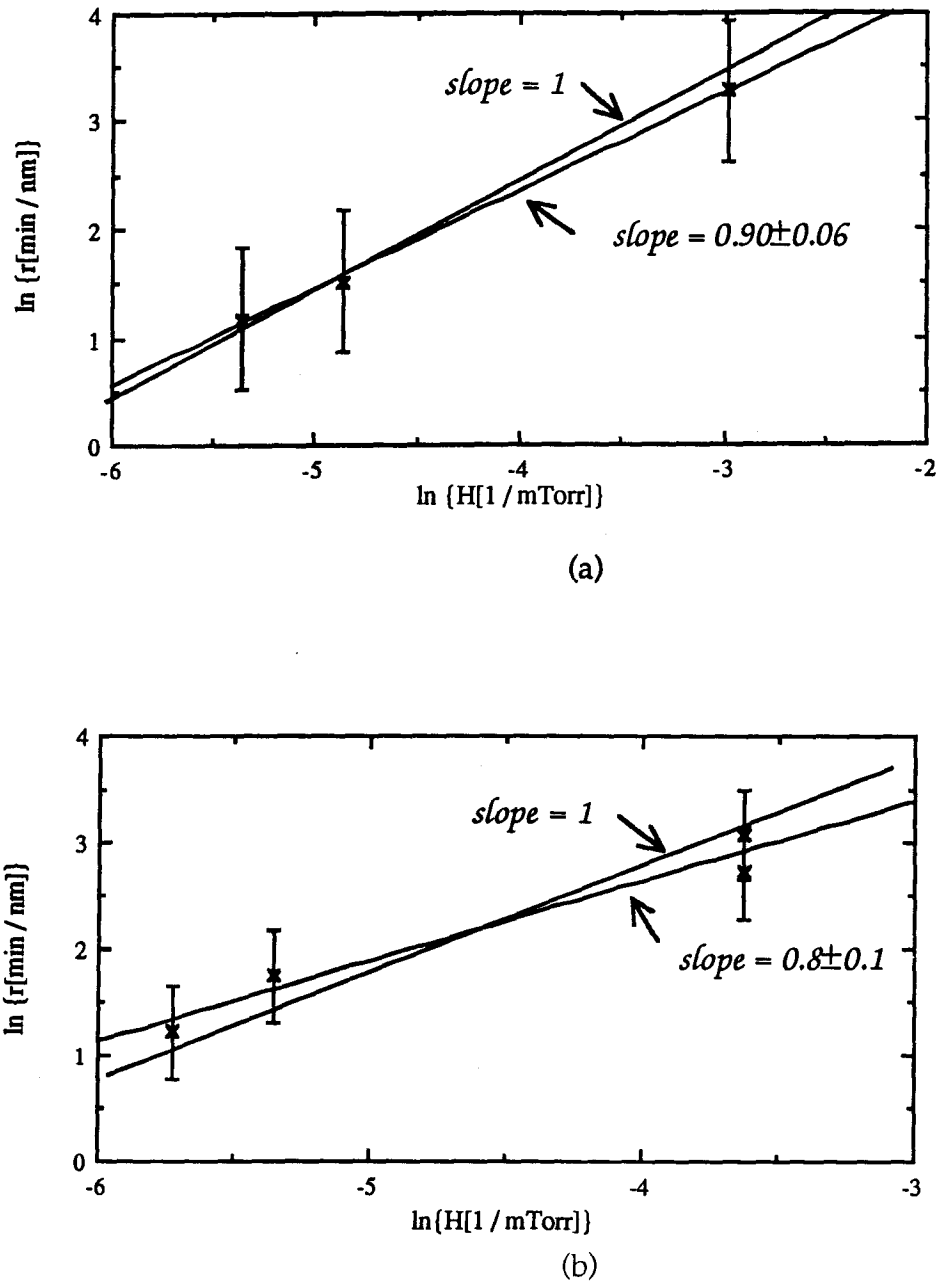

Figure 3-1. Plot of GaAs ln(etch rate) vs. ln(H atom partial pressure) at (a) 250 °C and (b) 280 °C to estimate the order of the reaction with respect to the H atom concentration.

(quoted errors are derived in the Appendix 1). Taking into account the fact that the H atom partial pressure uncertainty is suspected to be of order 25 %, the implications of the smaller, graphically determined errors associated with the reaction order determination can not be seriously considered. The more realistic 25 % uncertainty in the H atom partial pressure measurement brings the reaction order to unity within experimental error, or at least it is not evident the order of the reaction with respect to the hydrogen atom concentration differs from unity .

Reaction orders are frequently temperature dependent. In this narrow temperature range (between 250 °C and 280 °C) the two experimentally determined values of the order are the same, namely: unity.

To follow is a rate constant calculation which assumes the etching reaction is first order with respect to hydrogen atoms.

3.3 MEASUREMENT OF THE ABSOLUTE RATE CONSTANTS AND ACTIVATION ENERGY FOR ETCHING GALLIUM ARSENIDE WITH ATOMIC HYDROGEN

Assuming from the above discussion the reaction rate is first order with respect to H, the rate coefficeints (or constants) are related to the etch rate, r, via:

$$r = k_T[H]^1 = k_T[H]$$

where k_T is the rate coefficient at temperature T. k_T can also be related to the activation energy and the absolute temperature by the Arrhenius equation,

$$k_T = A \exp(-Ea/RT),$$

where the preexponential constant, A, and its uncertainty were found from the Arrhenius plot (see Appendix 2) to be,

$$A = 10^{5.7\pm0.7} \text{ nm min}^{-1} \text{ Torr}^{-1}.$$

The preexponential factor can be represented as a frequency factor, Z, through a simple conversion

$$Z = A \frac{\text{nm}}{\text{min Torr}} \times \frac{\text{cm}}{10^7 \text{ nm}} \times \frac{\text{min}}{60 \text{ s}} \times 2.21\text{x}10^{22} \frac{\text{molecules}}{\text{cm}^3}$$

$$Z = 1.96\text{x}10^{19} \frac{\text{molecules}}{\text{cm}^2 \text{ s Torr}}.$$

If the rate coefficient represents a simple elementary rate controlling reaction between a gas phase hydrogen atom and some unidentified surface species (perhaps GaH_2) to produce gaseous products, the preexponential cannot exceed the collision frequency of H atoms with the surface. In other words, the H atom supply rate at the surface must exceed the possible GaAs removal rate.

For atomic hydrogen at 360 °C, the limiting frequency factor per Torr of hydrogen atom pressure can be obtained from the relation,

$$Z = 3.513\text{x}10^{22} \text{ (M T)}^{-1/2} \text{ cm}^{-2} \text{ s}^{-1}$$

where T is the absolute temperature (633 K) and M is the atomic mass of hydrogen (1.008 g/mol). Upon substitution, we find,

$$Z = 1.39\text{x}10^{21} \text{ collisions cm}^{-2} \text{ s}^{-1} \text{ Torr}^{-1}$$

which is two orders of magnitude larger than than the "removal frequency" satisfying the aforementioned constraint leading us to conclude the rate constant that we measure is for a rate controlling elementary reaction of atomic hydrogen.

Hence the empirical temperature and activation energy dependence of the rate coefficient, k_T, for atomic hydrogen etching of (100) GaAs in the temperature range of this experiment (200 °C - 400 °C) is:

$$k_T = 10^{5.7\pm0.7} \text{ nm min}^{-1} \text{ Torr}^{-1} \exp(-29\pm7 \text{ kJ/mol})/RT.$$

The most direct way of experimentally determining the temperature dependent rate coefficients is to, assuming the reaction is first order in H, simply divide the etch rate at a temperature by the partial pressure of atomic hydrogen responsible for the etch. For example, an etch rate of 9.04 nm min^{-1} was observed at 360 °C while exposed to 5.46 mTorr of atomic hydrogen leading to:

$$k_{360°} = \frac{9.04 \text{ nm min}^{-1}}{5.46 \text{ mTorr}} = 1650 \text{ nm min}^{-1} \text{ Torr}^{-1}.$$

Table 3-3 contains all of the acquired GaAs temperatures, etch rates, H partial pressures and the corresponding rate constants. Not included in the table is the lowest temperature (180 °C) etch during which no measurement of the H atom concentration could be obtained. As the table infers the reaction rate increases with increasing temperature. An Arrhenius plot of the etch rate data (Figure 3-2) yields an activation energy for the etching of (100) GaAs with thermalised atomic hydrogen of 29±7 kJ/mol = 0.31±0.07 eV. This activation energy is slightly higher than that of Kishimoto *et al.* [43] but is difficult to compare directly for they quote no uncertainty.

3.4 POST-ETCH SURFACE DESCRIPTION

Upon discovery of a substantial reflectivity reduction at 632.8 nm during H atom etching of GaAs, it seemed a close look at the surfaces after etching may prove interesting. Subsequently, scanning electron microscopy was performed on some of the etched GaAs. In fact surfaces etched at the lowest temperatures, were unusually textured (Figure 3-3, below). Smoothness of the resulting surfaces seems to increase with temperature, as does the reflectivity at 632.8 nm relative to the reflectivity at 632.8 nm of the lower temperature, texturising etches.

The "dry" etching of GaAs with atomic hydrogen in the lowest temperature range (~ 200 °C) tends to culminate in gross surface texturisation presumably accompanied by enhanced optical absorbtion. As previouly described, a photoconductor was monitoring the specular reflection of a 632.8 nm helium neon laser off of the GaAs surface. Increased sample temperature during etching lead to lower levels of texturisation or the texturisation occured on a smaller scale. The

Kinetic Data

Temperature (°C)	Etch Rate (nm/min)	P_H (mTorr)	Rate Coefficient k_T (nm/min Torr)
229	4.3	9.79	439
235	3.2	7.79	405
250	4.5	7.74	584
250	3.2	4.68	684
278	3.4	3.27	1030
281	5.7	4.72	1210
360	9.0	5.46	1650

Table 3-3. The measured quantities: GaAs temperature, GaAs etch rate with atomic hydrogen, atomic hydrogen partial pressure during the reaction and computed rate coefficients.

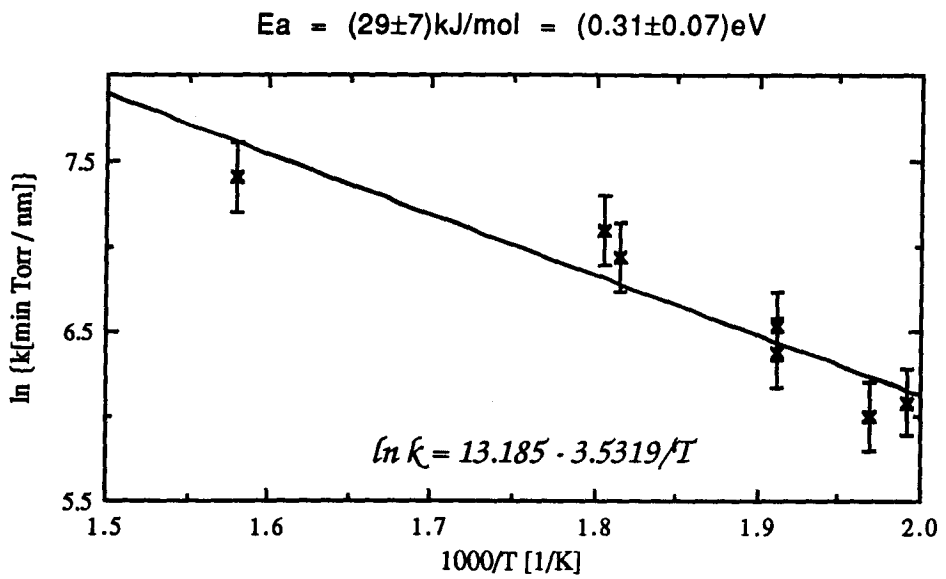

Figure 3-2 Arrhenius plot with standard error shown yielding determination of the activation energy for etching (100) GaAs with hydrogen atoms.

higher temperature etches (~ 300 °C) resulted in a smaller loss in reflectivity at 632.8 nm.

Scanning electron micrographs of the H atom etched surfaces have been studied in the 200 - 360 °C range. The micrographs clearly demonstrate that crystallographic etching is more pronounced at lower temperatures.

Of particular interest are the 180 and 205 °C micrographs of the etched (100) GaAs imaged from directly above the etched surface. Figure 3-3a and 3-3b are two perspectives of the same GaAs surface H atom etched at 205 °C. The axis of symmetry is apparent in both micrographs.

Figure 3-4a and 3-4b shows a reduction in the scale of the texturisation for 280 °C H atom etched GaAs relative to those etched in the 180 - 200 °C range.

Figure 3-5a and 3-5b demonstrate how smoothness improves for the mid to high temperature etches.

3.5 X-RAY PHOTOELECTRON SPECTROSCOPY RESULT

Although no gallium droplets were visible with the scanning electron microscope, results of X-ray Photoelectron Spectroscopy experiments performed at Surface Science Western, Ontario suggest the etched surfaces were Ga-rich. For a sample etched at 200 °C an As 3d to Ga 3d ratio of 0.31was obtained. This ratio of As to Ga on the surface, which would be unity if the surface was stoichiometric, indicated the etched sample surface was ~70 % gallium.

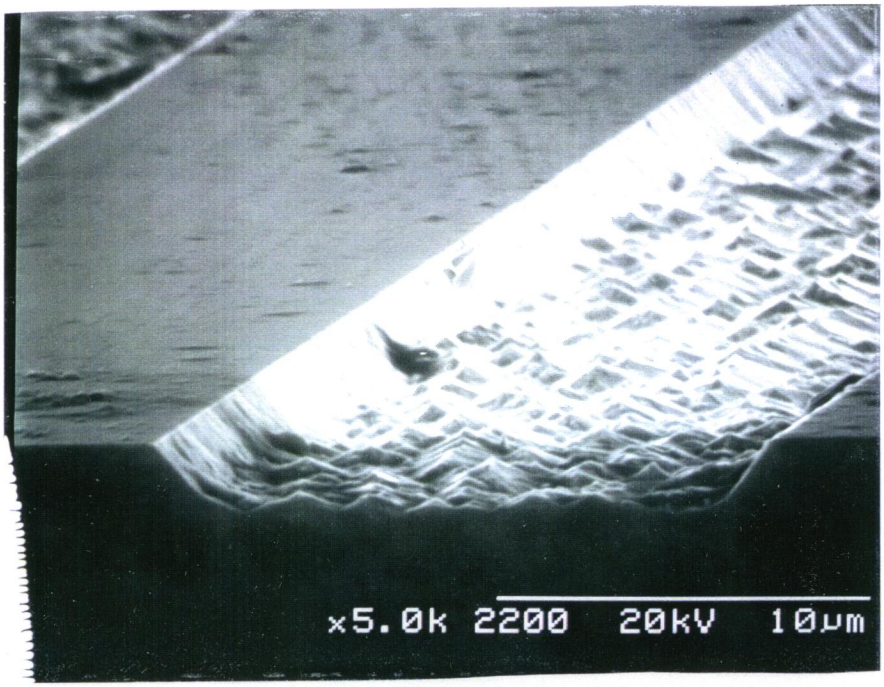

(a)

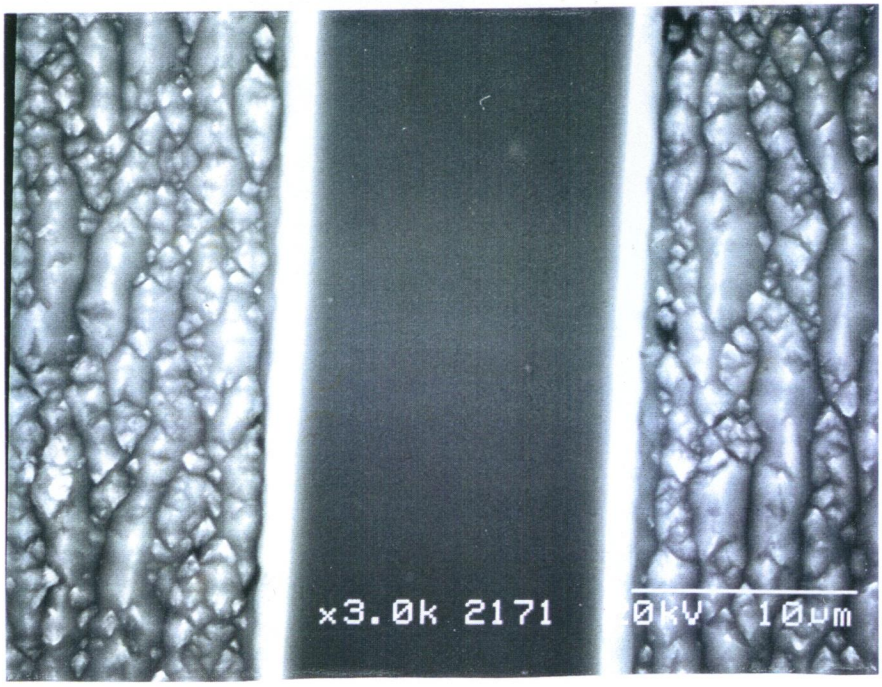

(b)

Figure 3-3. Scanning electron micrographs of H atom etched (100) GaAs at 205 °C as viewed from (a) the side and (b) the top.

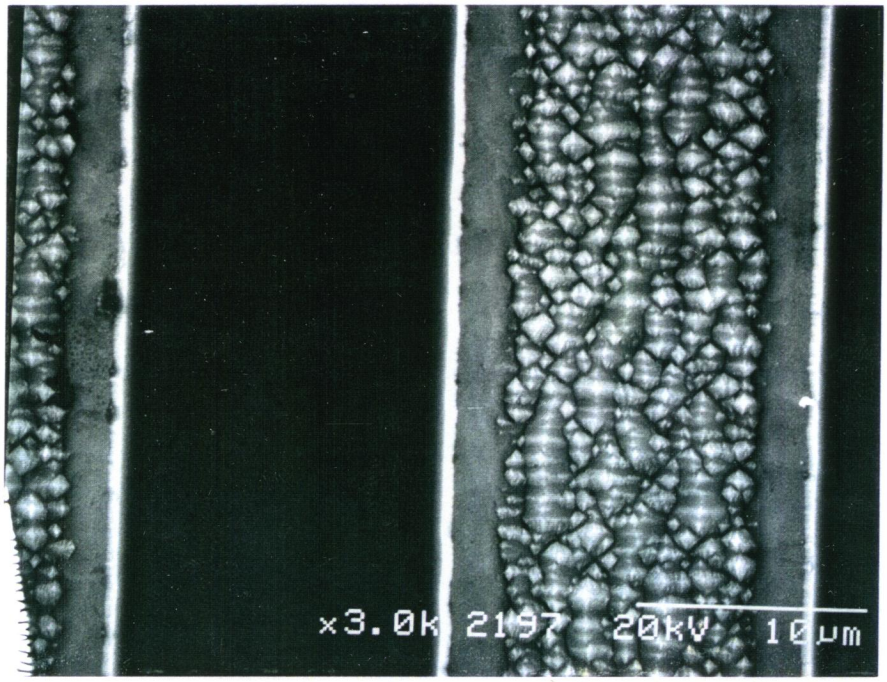

(a)

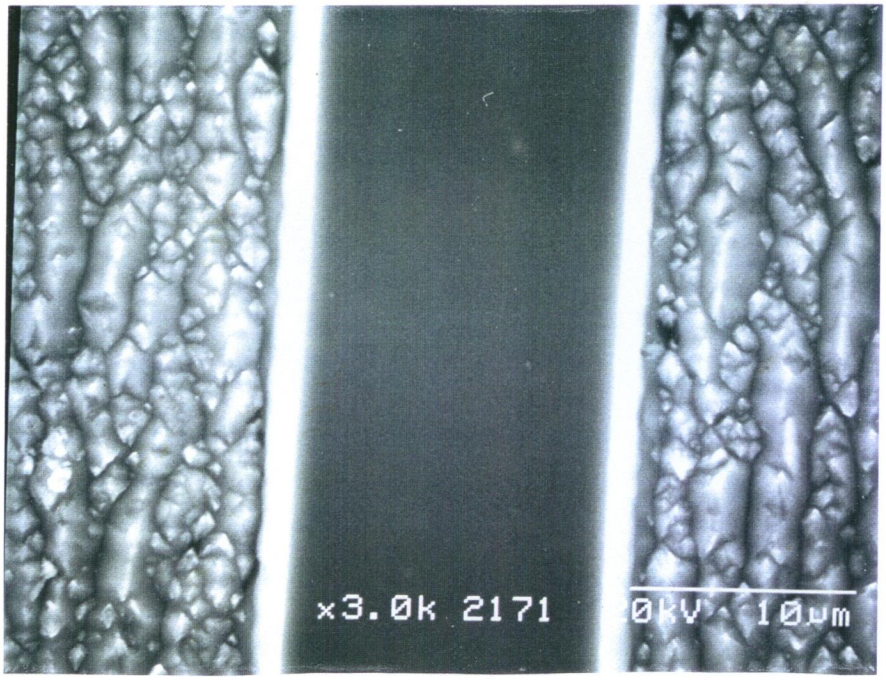

(b)

Figure 3-4. Scanning electron micrographs of (100) GaAs H atom etched at (a) 180 °C and (b) 205 °C as viewed from above.

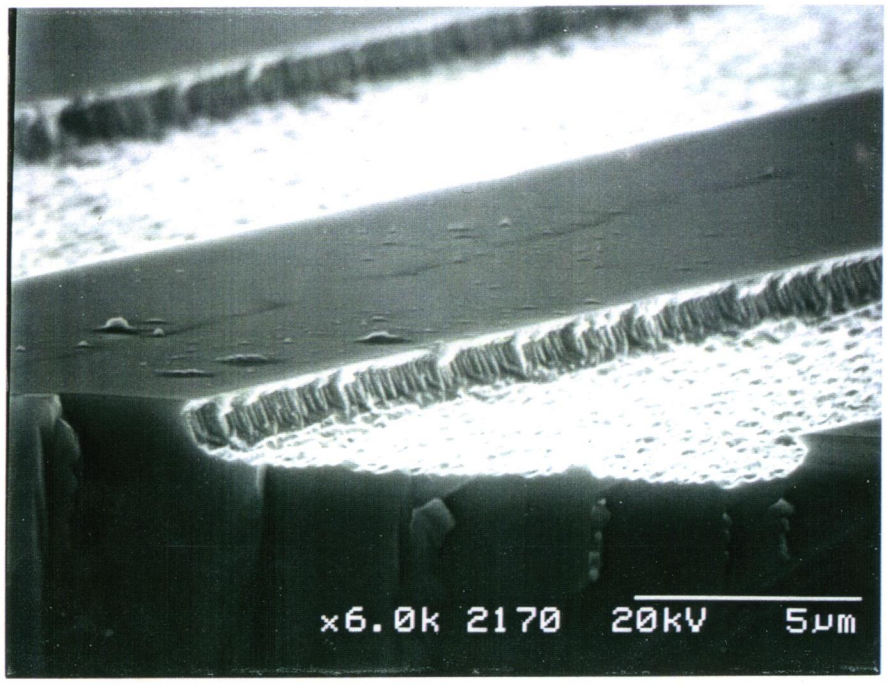

(a)

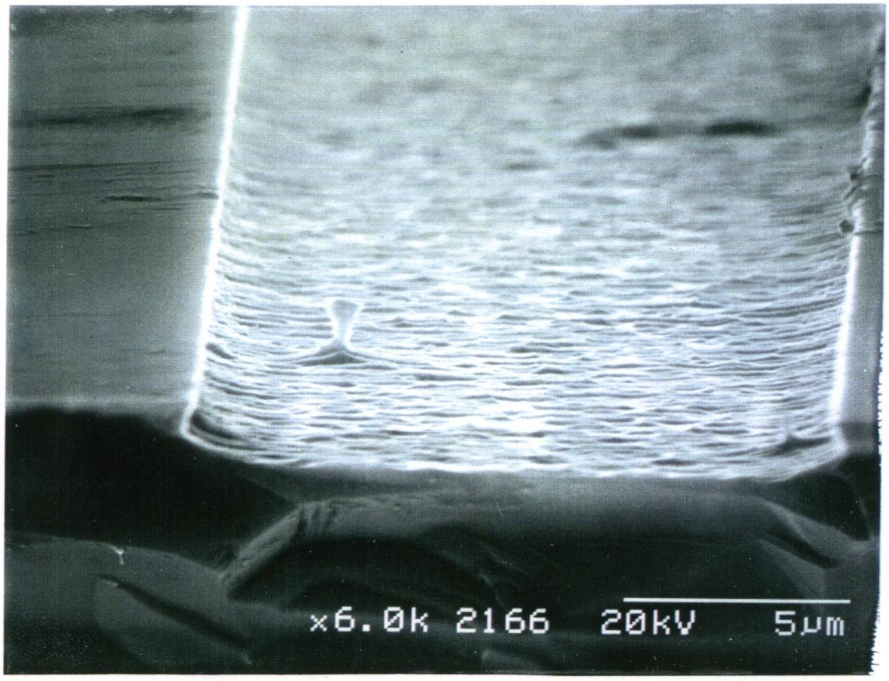

(b)

Figure 3-5. Scanning electron micrographs of (100) GaAs H atom etched in the mid to high temperature range: (a) 280°C and (b) 360 °C.

SECTION 4: DISCUSSION

4.1 ATOMIC HYDROGEN ADSORPTION ON SILICON AND GALLIUM ARSENIDE

Atomic H adsorption is known to occur on Si and GaAs[53]. According to recent band structure calculations[31] the presumably unreconstructed (100) GaAs surface turns out to be a metal without H adsorption. Both the gallium and arsenic surface dimers (considering the 2x4 reconstruction) are believed to be preserved[31], although buckled slightly, upon H adsorption. The added electron, in the case of GaAs, from the H effectively pushes some charge density down toward the adsorbate's bonds to the bulk.

Yamaguchi and Horikoshi[54] have in fact measured different activation energies for the desorption of arsenic from (100) GaAs depending on the reconstruction.

Unlike (100) GaAs, (100) Si is believed to break its dimer upon adsorption of atomic hydrogen[55]. The effect of the H adsorption on the Si-Si bonds (other than the broken dimers) should be much smaller (because the surface Si is again tetrahedrally coordinated) than the distortion imposed by H on GaAs resulting in little change of the energy needed to dissociate the Si.

Surface adsorbed H atoms may be diffusing into the bulk and bulk H atoms segregating to the surface[26].

4.2 ATOMIC HYDROGEN PLATELETS IN GALLIUM ARSENIDE

Platelets in GaAs exposed to atomic hydrogen may form due to the H - H interaction potential between bond center sites within the crystal[56]. It turns out the H - H interaction is repulsive for nearest neighbor H bond center sites and attractive for next nearest neighbor sites, repulsive....., attractive,..... and so on leading to a

condensed cluster of H oriented parallel to the {111} planes. These planes are assumed not to be of monolayer thickness but rather several planes coexist one, two, three or perhaps four next nearest neighbor bond lengths apart. So platelet thicknesses should be of order 15 - 50 Å and as mentioned previously hundreds of angströms in diameter.

4.3 ATOMIC HYDROGEN INDUCED CRYSTALLOGRAPHIC ETCHING

It has been well known for some time that different crystal planes have different formation energies associated with them. Covalent bonded solid surfaces, like GaAs, are considered to have free chemical or dangling bonds. Ge for example[57] has 1.25, 0.88 and 0.72 x 10^{19} dangling bonds per square meter on the (100), (110) and (111) surfaces, respectively. The relative etch rates of these planes in acid has been found to be 1.00, 0.89 and 0.62 respectively. This shows the {111} planes of Ge etch at 62% of the rate at which the {100} etch.

It is also worth noting that the work needed to create a unit area of surface under constant temperature and pressure is lower for more closely packed planes[57] The {111} are the most closely packed of the low index planes in GaAs, so one might expect this plane to form most easily.

Here we account for the anisotropy of the (100) surface etched with thermal H atoms. Upon examination of Figures 3-3 and 3-4[58] it is readily apparent that the protruding structures have symmetry along the trench (i.e. they are elongated along the trench, whereas they have little extent across the trench). We believe these figures, representing our lowest temperature etches achieveable, are of particular relevance since higher temperature etches lead to a loss of resolution of the crystallographic features. Perhaps low temperature (~200 °C) hydrogen atom etching of the (100) GaAs surface results in exposing either primarily $\{111\}_A$ or $\{111\}_B$ GaAs planes due to their different relative etch rates.

The planes exposed in the figures appear to be primarily {111}. Surface and extended bulk defects, due to their spatially enlarged charge distributions are often thought to be initiation "centres" for etching. Surface terminations of planar or line defects may provide initiation centres for etching and may feed H atoms into GaAs creating platelets along which etching may occur. Hence, platelet formation is a plausible explanation of the origin of the apparent texturisation of the H etched (100) GaAs surfaces.

SECTION 5: CONCLUSION

Thermalised atomic hydrogen continuously etches the (100) GaAs surface from temperatures as low as 180 °C with an activation energy of 0.31± 0.07 eV. The rate coefficient for the etching reaction over the 230 °C - 360 °C range can be described by,

$$k_T = 10^{5.7\pm0.7}\ \text{nm min}^{-1}\ \text{Torr}^{-1}\ \exp(-29\pm7\ \text{kJ/mol})/RT.$$

The rate constants were found to vary from 439 nm/min Torr at 229 °C to 1650 nm/min Torr at 360 °C and the reaction is close to first order in H. The lowest tempertaure etches left the (100) surface highly textured, exposing what appear to be mostly Ga-rich {111} planes.

SUGGESTIONS FOR FURTHER WORK

This study demonstrated etching (100) GaAs with atomic hydrogen in the lowest temperature range (~ 200 °C) leads to textured (100) surfaces possessing marked losses in optical reflectivity. Presently, solar cells are being fabricated from GaAs with the help of an antireflection coatings to minimize loss of incident light to reflection. Since H is the smallest of atoms which may be capable of creating the smallest of optically lossy voids in the near surface region of the GaAs, study of the extent to which the optical absorption increases after a low temperature H atom etch might be fruitful.

It also remains unknown to what degree the post-etched surface remains crystalline. Perhaps Raman scattering experiments could elucidate details of structural damage[59] or electron channeling experiments could be performed using a scanning electron microscope[60]to probe the crystallinity of the resulting surface.

Enquiry into the validity of the assumption that diffused atomic H is contributing to the etching reaction would certainly prove interesting. One could coat all but one surface with silicon nitride to presumably reduce the absorbed H atom flux. Alternatively, one could try saturating bulk GaAs at high temperature with atomic H and observe whether or not the etch continues after the source of H is removed.

The resulting surface morphology is sure to be strongly influenced by the atomic hydrogen concentration if etching is a result of H diffusion and subsequent platelet formation. Study of the H atom partial pressure dependence of the post-etched surface morphology may help solidify the interrelationship of these processes (i.e. etch over as wide a range of measurable H atom concentrations as possible).

Etching while simultaneously monitoring several of the diffraction maxima from the interferometer separately would help to determine the relevance of any "shadowing" contribution (i.e. a reduction in the intensity as the etch progresses due to reflection from the etched walls) to the interferogram arising from the finite depth of the etch trenches.

References

[1] S. J. Pearton, F. Ren, C. R. Abernathy, W. S. Hobson, T. R. Fullowan, R. Esagui, J. R. Lothian, Appl. Phys. Lett. **61** 586 (1992) and references therein

[2] N. M. Johnson, C. Doland, F. Ponce, J. Walker and G. Anderson, Physica B **170** 3 (1991)

[3] Paul C. Weakliem, Christine J. Wu and Emily A. Carter, Phys. Rev. Lett. **69** 200 (1992)

[4] S. J. Pearton, J. W. Corbett and M. Stavola, *Hydrogen in Crystalline Semiconductors*, p. 325, Springer-Verlag, 1992 and references therein

[5] see for example J. N. Heyman, J. W. Ager III, E. E. Haller, N. M. Johnson, J. Walker and C. M. Doland, Phys. Rev. B **45** 13 363 (1992)

[6] J. W. Corbett, J. L. Lindström and S. J. Pearton Mat. Res. Soc. Symp. Proc. **104** 229 (1988)

[7] A. Van Wieringen and N. Warmoltz, Physica **22** 849 (1956) in J. W. Corbett, J. L. Lindström and S. J. Pearton Mat. Res. Soc. Symp. Proc. **104** 229 (1988)

[8] N. M. Johnson, F. A. Ponce, R. A. Street and R. J. Nemanich Phys. Rev. B **35** 4166 (1987)

[9] J. Weber, Physica B **170** 201 (1991)

[10] W. B. Jackson and S. B. Zhang Physica B **170** 197 (1991)

[11] J. B. Boyce, N. M. Johnson, S. E. Ready and J. Walker, Phys. Rev. B **46** 4308 (1992)

[12] S. J. Feng and G. S. Oehrlein, Appl. Phys. Lett. **50** 1912 (1987)

[13] F. Lu, J. W. Corbett and L. C. Snyder, Physics Lett. A **133** 249 (1988)

[14] S. Nanarone, C. Astaldi, L. Sorba, E. Colavita and C. Colandra, J. Vac. Sci. Tech. A **5** 619 (1987)

[15] B. Clerjaud, F. Gendron, M. Krause and W. Ulrici, Phys. Rev. Lett. **65** 1800 (1990)

[16] R. Rahbi, D. Mathiot, J. Chevallier, C. Grattepain and M. Razeghi, Physica B **170** 135 (1991)

[17] N. M. Johnson, Physica B **170** 3 (1991)

[18] L. Pavesi, Solid St. Comm. **83** 317 (1992)

[19] L. Pavesi and P. Giannozzi, Phys. Rev. B 46 4621 (1992)

[20] L. Pavesi, P. Giannozzi and F. K. Reinhart, Phys. Rev. B **42** 1864 (1990)

[21] L. Pavesi and P. Giannozzi, Physica B **170** 392 (1991)

[22] R. G. Wilson et al. in J. H. Neethling, Physica B **170** 285 (1991)

[23] J. Chevallier, B. Machayekhi, C. M. Grattepain, R. Rahbi and B. Theys, Phys. Rev. B **45** 8803 (1992)

[24] E. M. Omeljanovsky et al. in S. J. Pearton, J. W. Corbett and J. T. Borenstein, Physica B **170** 85 (1991)

[25] J. M. Zavada et al. in S. J. Pearton, J. W. Corbett and T. S. Shi, Appl. Phys. A **43** 153 (1987)

[26] W. C. Dautremont-Smith, Mat. Res. Soc. Proc. **104** 313 (1988)

[27] K.C. Hsieh, M.S. Feng, G.E. Stillman, N. Holonyak, Jr., C.R. Ito and M. Feng, Appl Phys Lett. **54** 341 (1989)

[28] N. Caglio, E. Constant, J. C. Peasant and J. Chevallier, J. Appl. Phys. **69** 1345 (1991)

[29] J. H. Neethling, Physica B **170** 285 (1991)

[30] M. Stutzmann, J. -B. Chevrier, C. P. Herrero and A. Breitschwerdt, Appl. Phys. A **53** 47 (1991)

[31] Y. Miyamoto and S. Nonoyama, Phys. Rev. B **46** 6915 1992

[32] S. Nonoyama, Y. Aoyagi and S. Namba, Jpn. J. Appl. Phys. **31** 1298 (1992)

[33] G. Smolinsky, R. P. H. Chang and T. M. Mayer, J. Vac. Sci. Tech. **18** 12 (1981)

[34] R. P. H. Chang and S. Darack, Appl. Phys. Lett. **38** 898 (1981)

[35] R. P. H. Chang, C. C. Chang and S. Darack, J. Vac. Sci. Tech. **20** 45 (1982)

[36] A. Okubora, J Kasahara, M. Arai and N. Watanabe, J. Appl. Phys. **60** 1501 (1986)

[37] S. Sugata, A. Takamori, N. Takado, K. Asakawa, E. Miyauchi and H

Hashimoto, J. Vac. Sci. Tech. B **6** 1087 (1988)

[38]M. -C. Chuang, J. W. Coburn, J. Appl. Phys. 67 4372 (1990)

[39] I. Suemune, A. Kishimoto, K. Hamaoka, Y. Honda, Y. Kan and M. Yamanishi, Appl. Phys. Lett. **56** 2393 (1990)

[40] J. R. Creighton, J. Vac. Sci. Tech. A **8** 3984 (1990)

[41] J. A. Schaefer, V. Persch, S. Stock, Th. Allinger and A. Goldman, Euorophys. Lett. **12** 563 (1990)

[42] J. A. Schaefer, Th. Allinger, Ch. Stuhlmann, U. Beckers and H. Ibach, Surf. Sci. **251/252** 1000 (1991)

[43] A. Kishimoto, I. Suemune, K. Hamaoka, T. Koui, Y. Honda and M. Yamanishi, Jpn. J. Appl. Phys. **29** 2273 (1990)

[44] G. M. Mikhailov, P. V. Bulkin, S. A. Khudobin, A. A. Chumakov and S. Yu. Shapoval, Vacuum **43** 199 (1992)

[45] P. F. A. Meharg, Ph.D. Thesis, Dept. of Chemistry, University of British Columbia (1992), unpublished

[46] E. A. Ogryzlo, J. Phys. Chem. **65** 191 (1961)

[47] S. J. Pearton, J. W. Corbett and M. Stavola, *Hydrogen in Crystalline Semiconductors*, p. 8, Springer-Verlag, 1992 and references therein

[48] E. L. Tollefson and D. J. Le Roy, J. Chem. Phys. **16** 1057 (1948)

[49] Daniel W. Trainor, David O. Ham and Frederick Kaufman, J. Chem. Phys. **58** 4599 (1973)

[50] J. D. Strong and G. A. Vanasse, J. Phys. Radium **19** 192 (1958)

[51] Since the center to center spacing , a, of the nitride stripes is equal to twice the stripe width, b, all nonzero even orders vanish. Hence, due to our particular stripe geometry, the diffraction pattern consists of zero and odd order maxima only.

[52] R. J. Bell, *Introductory Fourier Transform Spectroscopy*, p. 208, Academic Press, 1972

[53] For an introduction see S. J. Pearton, J. W. Corbett and T. S. Shi, Appl. Phys. A **43** 153 (1987)

[54] H. Yamaguchi and Y. Horikoshi, J. Appl. Phys. **71** 1752 (1992)

[55] Z. Jing and J. L. Whitten Phys. Rev. B **46** 9544 (1992)

[56] S.R. Kreitzman, private communication.

[57] Richard A. Swalin *Thermodynamics of Solids,* p. 225, Wiley, 1972 and references therein

[58] Figure 3-6 has the same symmetry, however the mask orientation is perpendicular to that of Figure 3-3 and 3-4.

[59] see for example J.E. Maslar, S. R. Kisting, P. W. Bohn, I. Adesida, D. G. Ballegeer, C. Caneau and R. Bhat, Phys. Rev. B **46** 1820 (1992)

[60] D. C. Joy in *SEM Microcharacterization of Semiconductors,* p.69, ed. D. B. Holt and D. C. Joy, Academic Press, 1989.

APPENDIX 1: SLOPE UNCERTAINTY CALCULATIONS

The uncertainties in the estimated activation energy and reaction orders were calculated using the simple, conventional "Delta Y" method. The magnitude of both the activation energy, E_a, and the reaction order, x, are obtained graphically from slopes of logarithm plots since both parameters are exponents. The basic purpose of the "Delta Y" method is to approximate the error in the slopes of the plots and hence the uncertainty in the measurements of the physical quantities.

The name "Delta Y" presumably comes from the fact that this analysis proposes the fractional error in the slope, $\frac{\delta m}{m}$, is proportional to the average deviation of the data from the "best fit" line, δy, and inversely proportional to the range of the acquired data :

$$\frac{\delta m}{m} = \frac{2\delta y}{y_2 - y_1}$$

where m is the slope, δm is the uncertainty in the slope.

The quoted uncertainty in the activation energy will be computed here, using the above method. The quoted uncertainties in the reaction order with respect to the atomic hydrogen concentration can obtained similarly.

Since the technique is graphical one only needs a plot with a best fit (obtained here by Cricket Graph®) line to begin (see Figure A-1). δy is obtained by finding the average deviation of the data from the line along the ordinate (y-axis). In this example the average deviation, δy, of the data points parallel to the ln k - axis (see Figure A-1) is approximately 6.57 mm. The range of the data points, $y_2 - y_1$, in the same units is measured to be approximately 55 mm. The last quantity needed to estimate the uncertainty in the slope is the slope itself, m, obtained from the Curve Fitting program in Cricket Graph®. Using the above expression for the fractional error in the slope,

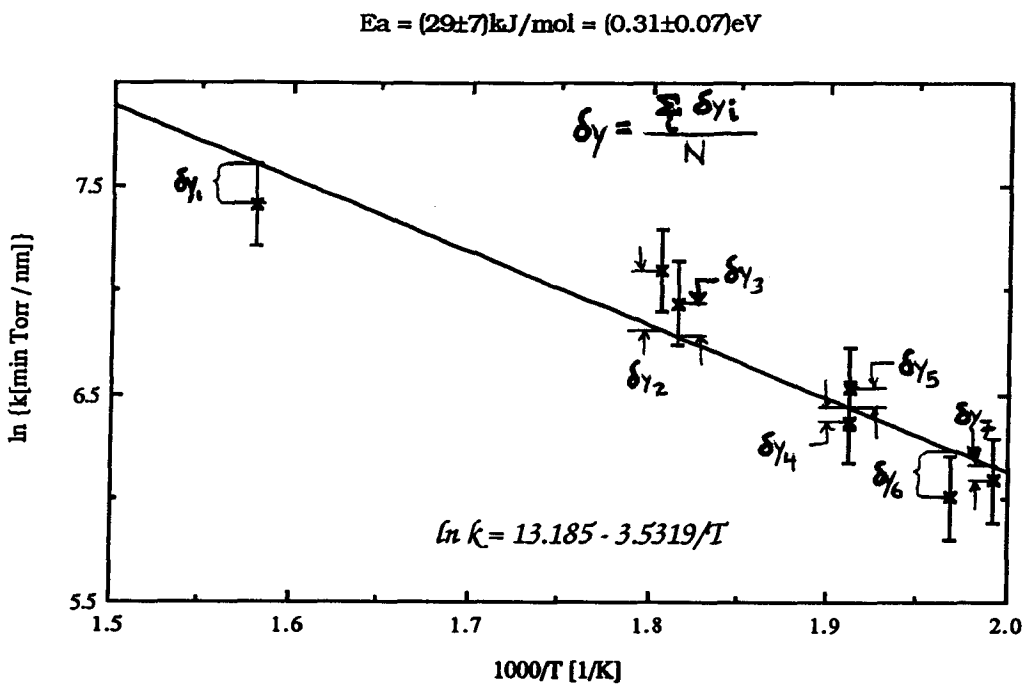

Figure A-1. Illustration of "Delta Y" method used for estimating the uncertainty in the activation energy associated with the reaction of hydrogen atoms with GaAs.

$$\delta m \approx \frac{(2)(6.57\ \text{mm})(3532\ \text{K})}{55\ \text{mm}}$$

$$\delta m \approx 841\ \text{K}$$

Now the slope with its uncertainty can be written as,

$$m \pm \delta m = (3532 \pm 841)\ \text{K}.$$

Next one needs the relationship between the slope and the activation energy. Assuming the rate constant, k, is related to the activation energy, E_a, via

$$k = A \exp(-Ea/RT)$$

where A is the preexponential related to the attempt frequency, R is the gas constant 8.314 J/mol K and T is the absolute temperature. Taking the natural log of both sides leads to an expression,

$$\ln k = \ln A - \frac{E_a}{R}\frac{1}{T}$$

which displays clearly that the relationship between the slope of a plot of ln k vs. 1/T and the activation energy is,

$$m = -\frac{E_a}{R}.$$

Solving for E_a,

$$E_a = -m\ R.$$

so,

$$\delta E_a = -\delta m\ R.$$

Finally, using the above value of the slope and its uncertainty for the hydrogen atom etching of GaAs,

$$E_a \pm \delta E_a = R(m \pm \delta m)$$

$$E_a \pm \delta E_a = (8.314\ \text{J/mol K})(3532\ \text{K} \pm 841\ \text{K})$$

$$E_a \pm \delta E_a = 29 \pm 7\ \text{kJ/mol}.$$

APPENDIX 2: PREEXPONENTIAL UNCERTAINTY ESTIMATE

The slope of the Arrhenius plot and its uncertainty for the etching of (100) GaAs with atomic hydrogen was obtained in Appendix 1. This slope and its uncertainty can aid in the determination of the preexponential factor, A and its associated error, δA.

The slope was found to be 3532 ± 841 K. The maximum and minimum slope would then be 4373 K and 2691 K respectively. These slopes were used to create linear functions enabling extrapolation of the upper and lower bounds for the experimentally determined preexponential factor (see Figure A-2).

For 1/T approaching zero the best-fit value of the natural logarithm of the rate coefficient (i.e. the y-intercept) was determined by Cricket Graph® polynomial Curve Fitting to be 13.2. This implies

$$\ln k \text{ (as T tends to } \infty) = \ln A \sim 13.2 ,$$

and

$$A = \exp(13.2) \sim 5.32 \times 10^5 \text{ nm min}^{-1} \text{ Torr}^{-1}.$$

The y-intercept for the maximum slope was found to be ~14.7 which leads to A_{max} ~ 2.39×10^6 nm min^{-1} Torr^{-1}. Similarly, the y-intercept for the minimum slope was found to be ~11.3 which leads to A_{min} ~ 8.40×10^4 nm min^{-1} Torr^{-1}.

To express this preexponential and its uncertainty in conventional notation we want to write it as 10^{γ} nm min^{-1} Torr^{-1},

$$\exp[(\ln k)_{max}] = e^{14.688} = 10^{\gamma_{max}}$$

and

$$\exp[(\ln k)_{min}] = e^{11.339} = 10^{\gamma_{min}}$$

which yields $\gamma_{max} = 6.38$ and $\gamma_{min} = 4.92$.

The preexponential with its associated uncertainty will be written

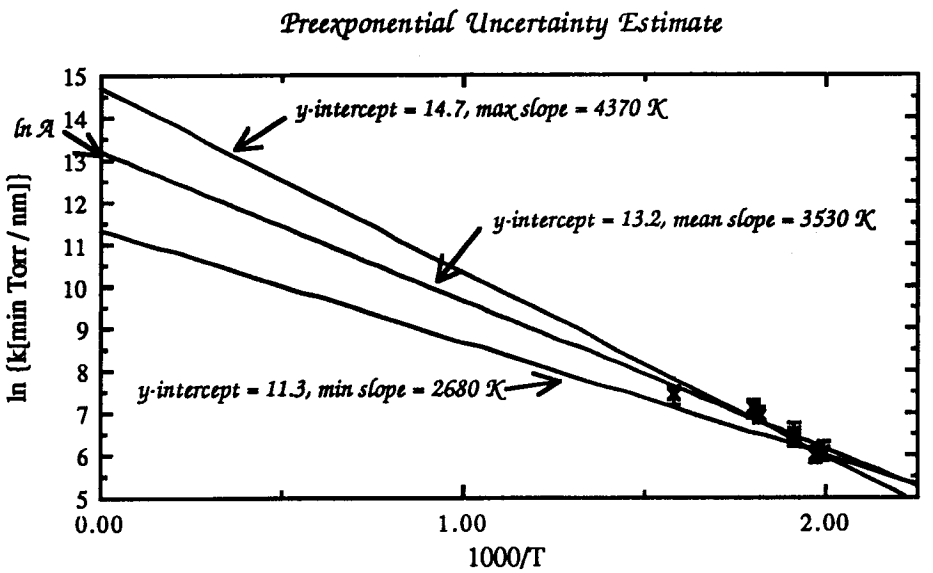

Figure A-2. Extrapolation to large T and resulting Arrhehnius preexponential with uncertainty determined by the maximum and minimum slopes of the Arrhenius plot for H atom etching of (100) GaAs.

$$10^{(\gamma \pm \delta\gamma)} \text{ nm min}^{-1} \text{ Torr}^{-1},$$

where,

$$\delta\gamma = \frac{\gamma_{max} - \gamma_{min}}{2}$$

$$\delta\gamma = 0.73.$$

Finally, the preexponential can be written:

$$A = 10^{5.7 \pm 0.7} \text{ nm min}^{-1} \text{ Torr}^{-1}.$$